

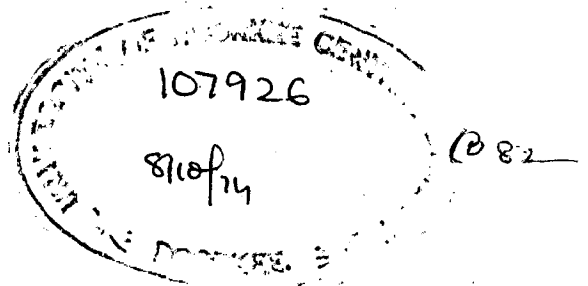
✓ F-74
CHA

LIQUID FLUIDIZATION IN TAPERED VESSELS

A DISSERTATION
submitted in partial fulfilment of the
requirements for the award of the Degree
of
MASTER OF ENGINEERING
in
CHEMICAL ENGINEERING
(EQUIPMENT & PLANT DESIGN)

By
ISHWAR CHANDRA

RECEIVED
1975



DEPARTMENT OF CHEMICAL ENGINEERING
UNIVERSITY OF ROORKEE
ROORKEE (INDIA)

May 1974

ABSTRACT

Recent work involves the study of liquid fluidization in tapered vessels with tapering ranging from 10 to 120°. Coarse and solid particles (Glass beads, Quartz and Calcite) have been used for studying the effect of physical properties of the material, bed weight and cone angle on fluidization characteristics. Graphs plotted between pressure drop and liquid flow rate show the expected behaviour and trend. Following correlation has been proposed for the determination of pressure peak,

$$\left(\frac{\Delta P}{\Delta P_0}\right) = 1.02 \times 10^{-3} \left(\frac{D}{D_0}\right)^{1.63} \left(\tan \frac{\alpha}{2}\right)^{-1.23} \left(\frac{D_p G}{\mu}\right)^{0.712}$$

It has been observed that smooth fluidization occurs only in lower cone angles i.e. 10, 15 and 20°, for the materials studied. In 30 and 45° cones particle movement is similar to the one observed in open bed. In overtopped vessels of cone angles greater than 45° and upto 120° mixing of solids is confined to the central part of the bed only with thick particle layer remaining stationary at the vessel wall.

ACKNOWLEDGEMENT

The author wishes to express his deep sense of gratitude to Dr. N. Gopal Krishna, Professor and Head, Chemical Engineering Department, University of Roorkee, Roorkee for his kind help and guidance during the course of the work. Author is further indebted to the Professor for providing necessary laboratory, fabrication and other facilities within and outside the department.

The author is grateful to Dr. P.S. Panesar, Associate Professor for providing fabrication facilities, time to time help and valuable suggestions regarding this thesis.

Thanks are due to Sri N.J. Rao, Reader, Sri Surendra Kumar, Lecturer, Chemical Engineering Department, University of Roorkee, Roorkee for their kind help and suggestions.

I am also thankful to various laboratories, fabrication section staff and others who contributed a lot in completion of this work.

Ishwar Chandra.
(ISHWAR CHANDRA)

C O N T E N T S

	Page No.
ABSTRACT	1
ACKNOWLEDGEMENT	11
CONTENTS	111
CHAP. I INTRODUCTION	1
1.1 - Introduction to Fluidization Phenomenon	1
1.2 - Comparative study of Fluidization in Cylindrical and Tapered Vessels.	5
1.3 - Fluidization in Tapered Vessels	8
CHAP. II LITERATURE REVIEW	11
2.1 - Fluidization of Solids by Gas Stream	11
2.2 - Liquid Fluidization of Solids	17
2.3 - Pressure Drop in Conical/Tapered vessels.	19
2.4 - Bed Expansion in Tapered Beds	22
2.5 - Design of Tapered Beds.	23
CHAP. III EXPERIMENTAL SET UP AND PROCEDURE	27
3.1 - Experimental Set up	27
3.2a. Fluidizing Columns (tapered vessels)	27
3.1b. Grid Plate	28
3.1c. Calming section	29
3.2 - Experimental Procedure	29
CHAP. IV EXPERIMENTAL DATA, RESULT AND DISCUSSIONS	31
CHAP. V CONCLUSIONS	73
REFERENCES	
NOMENCLATURE	
APPENDIX	

CHAPTER I

INTRODUCTION

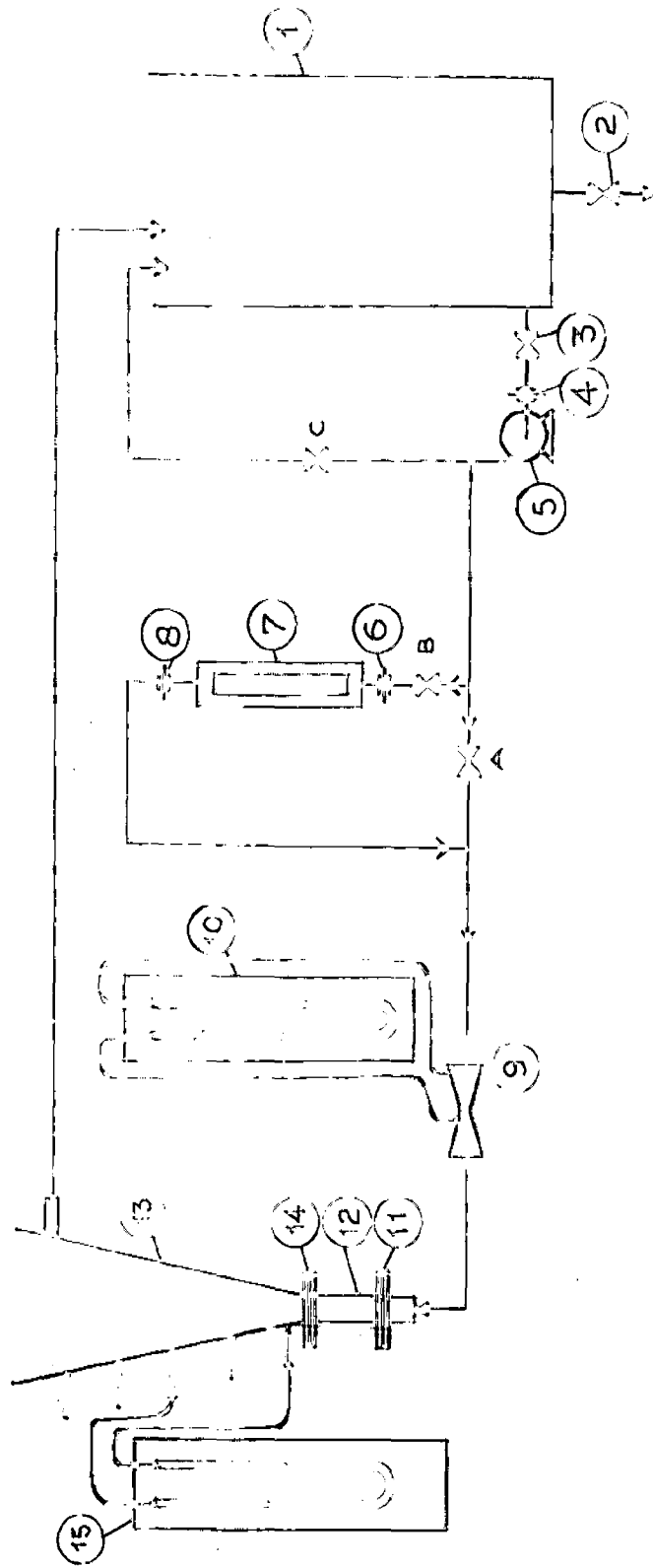
1.1 INTRODUCTION TO FLUIDIZATION PHENOMENON:

Fluidization is the operation by which fine solids are transformed into a fluid like state through contact with fluid stream.

When fluid is passed upward in a bed of closely sized granular solids, a pressure gradient is required to overcome friction. In order to increase the rate of flow, a greater pressure gradient is required. At low flow rates, fluid merely percolates through the void spaces between stationary particles. With increase in flow rate, particles move apart and a few are seen to vibrate and move about in restricted region. This is 'expanded bed'. At still higher velocities, a point is reached when the particles are all just suspended in the upward flowing stream. At this point the frictional force between a particle and fluid counter-balances the weight of the particle, the vertical component of the compressive force between adjacent particles disappears and the pressure drop through any section of the bed about equals the weight of the bed in that section. The motion of the solids is created at superficial velocities far below the terminal free settling velocities of the solid particles and constitutes the beginning of the fluidization. This is point of 'incipient or minimum fluidization'. The process is approximately equivalent to the inverse of hindered settling.

The precise behaviour of a mass of fluidized solids depends on the particle size and the nature of the fluid. When the fluid is liquid, fluidization begins as a gentle rocking or oscillation of the solid particles. In the fully fluidized bed, the particles move in random directions through all parts of the liquid. There are strong transient currents in the bed with many particles travelling temporarily in the same direction, but in general particles move as individuals. Gross flow instabilities are damped and remain small and large scale bubbling or heterogeneity is not observed under normal working conditions. With further increase in the liquid rate a smooth progressive expansion of the bed results until each particle behaves as an individual and is unhindered as a freely settling body by the action of any other solid particle. This entire process is known as 'particulate fluidization'.

When the fluid is a gas, the action in the bed is what different and is strongly influenced by the particle size. Under conditions for good fluidization (with particles of the proper size and density) some of the gas travels through the bed between individual particles, but much of it travels through in 'bubbles' or 'pockets' containing almost no solids. At the bed surface the bubbles break, 'splashing' individual particles or



- | | | |
|-------------------------|-------------------------------|--------------------------------|
| A, B, C - CONTROL VALVE | 7. ROTAMETER | 13. TAPERED VESSEL |
| 1. STORAGE TANK | 9. VENTURIMETER | 14. GRID PLATE |
| 2, 3. GLOBE VALVE | 10. Hg ₂ MANOMETER | 15. CCl ₄ MANOMETER |
| 4, 6, 8. UNION | 11. SUPPORT PLATE | |
| 5. CENTRIFUGAL PUMP | 12. CALMING SECTION | |

streamers into the space above. In the bed itself the particles move in distinct aggregates which are lifted by the bubbles or which move aside to let the bubbles past. A fluidizing action of this kind is known as 'aggregative fluidization'.

When particles are fluidized in a tall narrow vessel a phenomenon known as 'slugging' may occur. Bubbles of gas tend to coalesce and grow as they rise through the fluidized bed. The rate of growth depends on the size and density of the particles; it is rapid when the particles are large and heavy, slow when they are small and light. If a vessel that is small in diameter contains a deep bed of solids, the bubbles may grow until they fill the entire cross-section of the vessel. Successive bubbles then travel up the vessel, separated by the slugs of the solid particles. Operation is erratic and unstable.

A typical variation of pressure drop with superficial velocity is shown in Fig. 1 where the logarithm of the pressure drop is plotted against the logarithm of fluid velocity. The straight line from A to B represents the variation of the pressure drop through the bed with fluid velocity during the period of fixed bed operation when no motion of the particles occurs. Fluid merely percolates through the void spaces between stationary particles and the pressure drop is given by Kozeny-caman

equation. Eventually the pressure drop equals the force of gravity on the particles (Point B). Bed has become unstable now and a minor movement and re-adjustment of the particles in the bed begin to take place to offer the maximum cross-sectional area for flow. Bed expands slightly with the grains still in contact. The change in the structure of the bed produces a deviation from the simple relationship between the pressure drop and the velocity shown in the section A to B. Instability of the bed continues as the velocity is increased, until at point C the loosest arrangement of particles in contact is established. With any further increase in the velocity of flow some of the particles in the bed are no longer in permanent contact with one another and becomes continuously agitated. This point 'C' is known as the point of incipient fluidization. At this point of fluidization the bed begins to expand with increasing fluid velocity thus more and more particles losing contact with others. At point 'D' fluidization is complete and all the particles are in motion. From point 'C' to 'D' there is sudden though slight fall in the pressure drop due to unlocking of particles with each other. Further increase in fluid velocity beyond the point 'D' are attained by relatively slight increase

in pressure drop merely that required to overcome the increase in frictional losses between fluid, suspended solids and walls of the container. Particles move more and more vigorously, swirling about and travelling in random directions. The contents of the tube per se resemble a boiling liquid.

The linear velocity of the fluid between the particles is much higher than the velocity in the space above the bed. Consequently nearly all the particles drop out of the fluid above the bed. Even with vigorous fluidization only the smallest grains are entrained in the fluid and carried away. As fluid velocity is further increased the porosity of the bed rises, the bed of solids once expands, and its density falls. Entrainment becomes appreciable, then severe, then complete. At point 'E' all the particles have been entrained in the fluid, the porosity approaches unity, and the bed as such has ceased to exist. The phenomenon then becomes that of the simultaneous flow of the phases. From point 'D' to 'E' and beyond pressure drop rises with fluid velocity very slowly.

1.2 COMPARATIVE STUDY OF FLUIDIZATION IN CYLINDRICAL AND TAPERED VESSELS

When fluidization is carried out in cylindrical vessels, a usual practice, solids mixing rate in longitudinal direction is quite severe when they are fluidized by

gas stream. This severe solids mixing is responsible for increased heat and mass transfer rates between the two phases i.e. solids and the fluid stream due to increased bed turbulence but at the same time creates solids back - mixing in the same direction. Both increased bed turbulence and solids back mixing may not be desirable in some cases for example in case when solids are under use as catalyst, this extreme bed turbulence may result in a continuous attrition of solids and thus less of catalyst as fines which will be carried out of the bed along with rising gas stream. In case of continuous processing of solids, where it is desirable that each solid particle should spend the same length of time in the bed as any other i.e. solids should move along with rising fluid stream in a piston like manner. Back mixing of solids in the bed will make that some solid particles will be grossly over-reacted whilst others may well pass through unreacted. In such cases it is advantageous to have reduced degree of mixing of solids in longitudinal direction but still retaining all the other desirable properties of the fluidization.

The back mixing of solids, as created by severe solids mixing rate is supposed to be reduced if fluidization is either carried out in long narrow tube with high L/D ratios or in 'multistages'. It has been observed that

if fluidization is carried out in deep beds with high L/D ratios it is quite non-uniform. Since in such beds pressure drop is quite satisfactory and being a compressible fluid gas goes on expanding as it passes through the bed thus there is a consequent rise in its velocity. When the upper portion of the bed is made to fluidize satisfactorily it has been found that lower portion of the bed is not fluidized at all while when the gas velocity at the base or distributor corresponds to the U_{mf} value i.e. bottom is made to fluidize satisfactorily the upper part of the bed is slugging badly. This is specially serious for uniformly sized large and dense solid particles where it is difficult to fluidize the bed at all.

If fluidization is carried out in tapered/conical vessels with such a taper that superficial gas velocity is more or less constant around U_{mf} value as the gas rises up through the bed, the whole bed can be fluidized uniformly through out its height. This is only true for deep bed of dense material or with uniformly sized coarse/dense materials. Solids mixing rate which was severe in cylindrical beds is reduced much in such vessels, still retaining other desirable important properties of the fluidized bed. This may also be possible because of the major portion of the gas which flows

through the bed as large practically solid free gas bubbles while the bed solids are suspended by a relatively slow moving gas.

In case of liquid fluidization it has been observed that when the bed is satisfactorily fluidized the bed expansion is not uniform. Porosity of the bed goes on increasing from bottom to the top. Further the interface at the top of the fluidized bed is not clear and distinct.

The another advantage of tapered vessel is that mixed sizes can be fluidized well, the fines or lighter being at the top while the coarser or denser at the bottom with intermediates in between. Thus attrition of solids as fines along with rising fluid stream is eliminated completely which is advantageous for catalytic reactions.

1.3 FLUIDIZATION IN TAPERED VESSELS:

When fluidization occurs in conical vessels tapering downward there is a considerable pressure peak at the limit of stability. This peak is much larger than at on set of fluidization in an apparatus with constant cross-section and is due to conical form of the bed. In some experiments of Golperin (1960)⁸ the pressure drop before the on set of fluidization was two to three times greater than the value established after the limit of stability. In a conical apparatus the bed passes into

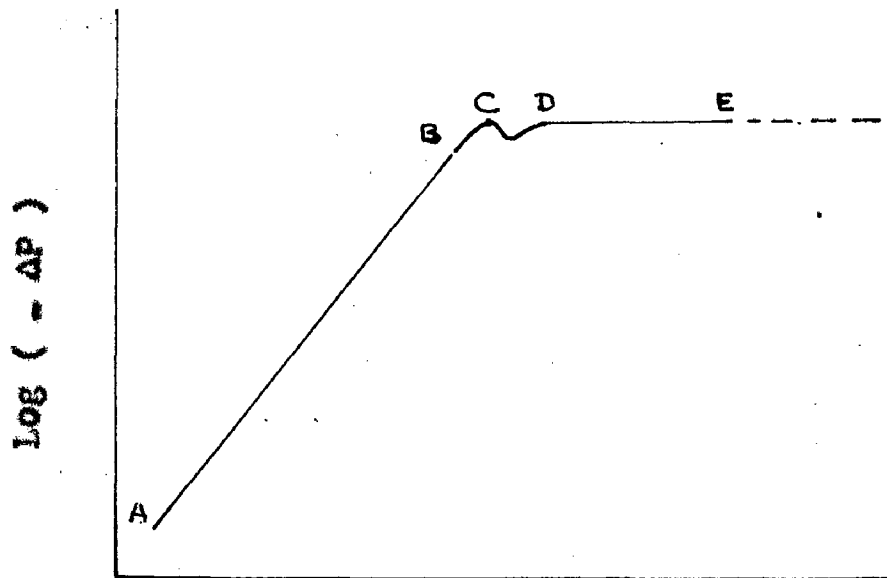
the fluidized state only after fluidization of its upper portion. Since at this time the gas velocity in the lower and middle portions of the bed are considerably greater than the critical fluidization velocities, the pressure drop in the stationary bed portions increases rapidly compared with that at the limit of stability in a cylindrical bed of the same height. Immediately beyond the limit of stability the pressure drop falls to approximately the usual theoretical value, equal to the product of the bed density and its height, regardless of its configuration in the same way that the hydraulic pressure on the bottom of a vessel does not depend on its shape.

$$\Delta P = (1 - \epsilon) (\rho_s - \rho_f) \frac{\partial}{\partial c} \cdot L = \frac{W_{net}}{A_{avg}} \quad (1)$$

Here L is the bed height, W , the bed weight and A_{avg} the average bed cross-sectional area.

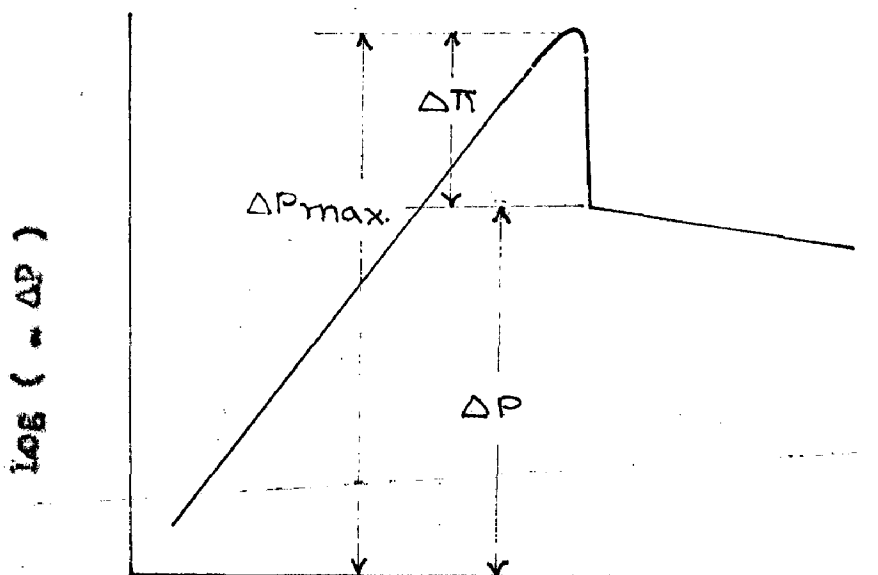
As the fluid velocity is further increased the pressure drop does not remain constant but, in contrast to the cylindrical bed, begin to fall. The reason being that as the fractional voidage ' ϵ ' increases, the bed height more or less do not increases with the same speed and thus the product $L(1 - \epsilon)$ goes on decreasing. (Fig. 1.2)

Experiments have revealed that in conical vessels the point of incipient fluidization is not as clear cut as in cylindrical vessels. Further, as the upward flow of fluid through the fixed bed of particles in a conical vessel is increased from zero, a compacting effect is noted. This effect is seen well below the point of incipient fluidization. The explanation appears to be that the particles near the bottom of the bed can experience a substantial upward drag force, due to relatively large velocity of the fluid near the bottom of the bed. The upward drag force can be larger than the force of gravity on the particles. At the same time, the velocity near the top of the bed is still relatively small, so the force of gravity on particles near the top of the bed is larger than the upward drag force exerted on them by the fluid. The resultant force on the particles near the bottom is upward and the resultant force on the particles near the top is downward. The bed height reaches a minimum value due to this compaction effect and a minimum observed porosity is thus realized.



log of superficial fluid velocity, v

FIG. 1.1 - PRESSURE DROP VS. FLOW RATE CURVE FOR A BED OF CLOSELY SIZED PARTICLES



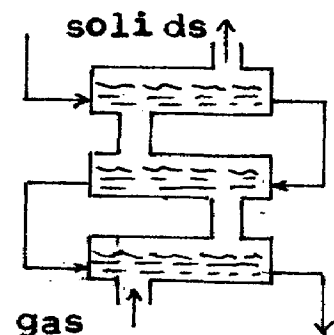
log of superficial fluid velocity, v

FIG. 1.2 - PRESSURE DROP VS. FLOW RATE CURVE FOR SOLID PARTICLES IN A TAPERED VESSEL

2. LITERATURE REVIEW

2.1 FLUIDIZATION OF SOLIDS BY GAS STREAM:

As already stated that in case of gas fluidization solids mixing rate in vertical direction is quite poorer in cylindrical beds. Brotz (1952)² and Roman (1953)³ stated that the mixing rate increases with increasing fluid velocity. Most of the mixing of solids in the fluidized bed occurs by the bulk movements of the solid material. Such bulk movements are generally associated with eddies in liquid fluidized beds and with bubbles in gas fluidized systems. This poorer mixing in longitudinal direction causes back mixing of solids in the bed. Experimental 8, 9, 10 works to know the residence time distribution of solid particles in a continuously fed gas fluidized bed have shown that solids behave approximately as the contents of a continuously stirred tank or perfectly mixed vessel. Spread of residence time is very wide indeed. So that the wide range of residence time distribution in a continuous gas fluidization column may be reduced, either fluidization is to be carried out in multistages¹¹ with a narrow range of solids residence time in each with overall counter current flow of gas and solids (Fig. 2.1) or to make the bed very deep in relation to its diameter in order to make mixing of the upper end



(Fig. 2.1)

lower regions of the bed more difficult. But this leads to the non-uniformity of fluidisation quality.

If deep beds are employed in cylindrical vessels the pressure drop between bottom and top of the bed, which is needed for the gas flow to occur through the packed bed and to overcome the resistance offered by the solids in the passages and thus fluidize the bed, becomes satisfactory. The gas velocity increases considerably due to the gas expansion as gas passes through the bed from bottom to top. This means that if the gas velocity is only made sufficient to give normal fluidizing conditions in the upper regions of the bed, the base of the bed will be completely static. If the gas velocity is increased until fluidisation occurs immediately above the support plate at the bottom of the bed, then the bed is violently agitated at the top, and transport of bed material may occur.

It was originally suggested by Omas and Furukawa (1963)²¹, for liquid fluidized beds, that a possible solution to the problem of smooth operation of deep beds would be to increase the bed cross-sectional area upwardly through the bed so that increase in gas volume could be accommodated i.e. to construct a bed tapering

towards its base. Thus uniformly expanded bed, in case of liquid fluidization, can be achieved. The first such bed to be constructed and operated was that of Levey et. al (1960)¹ who were investigating the possibilities of a fluidized bed reactor for the conversion of Uranium Oxide to Uranium Fluoride by fluidization with Hydrogen Fluoride gas mixed with 5% Nitrogen as a diluent to moderate the reaction and carry away the heat. Spheriodally shaped UO_3 particles in size range 20-40 mesh were fluidized in 4-5" cylindrical tubes and for bed heights above two feet fluidization was highly non-uniform with violent bed eruptions and inefficient contacting of the fluid. Fluidization was observed to begin at the upper surface of the bed and proceeded downward through the bed as the inlet gas velocity was raised and when the gas velocity was sufficient to fluidize the bed completely the upper portion of the bed was slugging. Since the superficial gas velocity increases considerably along the bed owing to the expansion of the gas (the pr. drop being approximately 1.75 psi/ft) the bubble volume increases steadily along the bed, and thus deeper the bed and higher the particle density or size, the greater is the tendency of the bed to slug. Bed expansion was

quite high and a much higher velocity is required to fluidize the whole bed, than for a shallow bed.

To compensate for the gas expansion thus to have constant superficial gas velocity along the bed, they employed a suitably tapered tube. The angle of taper for the ideally fluidized bed was as calculated out, for conical vessels:

$$\alpha = \tan^{-1} (a_0 \rho_B / 2p_b) \quad (2)$$

Here a_0 is the distance normal to the longitudinal axis of the column between tapered sides. ρ_B is bulk density of the bed and p_b is pressure at the inlet to the bed.

In such beds it was noted that pressure drop-flow rate curves are like those ordinarily encountered in fluidized beds, a linear portion before the bed is fluidized and thereafter a horizontal linear portion. Thus quite uniform fluidization was seen taking place. All the properties normally associated with the fluidized state, such as flow ability of the bed and good heat and mass transfer were retained and the bed expansion was reduced, gas bobble formation was largely suppressed and most important of all, the amount of mixing between the upper and lower regions of the bed was reduced by

at least an order of magnitude. It was noted that at velocities substantially above the minimum, bubbles do appear but they do not coalesce and in many cases disappear before reaching the upper surface.

According to Romero and Johanson (1962) the reduced rate of mixing of solids is caused by operating ~~rate-of~~ close to the minimum fluidizing velocity.

Sutherland (1961)⁴ carried out mixing rate experiments using a tapered bed of copper shot, sized between 30-52 Mesh. Nickel spheres of the same size and density acted as a tracer material which were added (about 1% of the bed weight) from the top while the bed was under just fluidization state and then increasing the gas velocity to the desired values. Qualitatively, the curves of Nickel concentration against time for various probe locations showed that vertical solid mixing rate was greatly reduced in the tapered beds. It was also shown that this effect is found only with deep beds of dense materials and only at flow rates less than 30% above the MFV and to bed heights greater than 2 feet. Sutherland also observed like Levey et. al¹ that particle movements and bubbling in untapered beds began at the top of the bed as the air rate was increased and that by the time particle movements was observed at

the base, the top was slugging violently. In tapered beds he observed that the fluidization at lower velocities was more even with bubbles appearing in the lower as well as in the upper part of the bed. Once the flow rate reached $1.2 - 1.3$ times of U_{mf} , however, the whole bed began to slug and to appear very similar to the corresponding non-tapered beds. In contrast to cylindrical beds, a more precise value of U_{mf} was obtained for tapered beds. Thus main effect of tapering would appear to be the stabilizing of the just fluidized state through out the depth of the bed.

Later work of Sutherland and Howe (1964)⁵ was directed at elucidating the mixing mechanism. A bed of copper shots was overlaid with a Nickel shot layer and fluidized for varying periods. It was concluded that with out bubbles in the bed there was no mixing and the range of flow rates in which the bed was fluidized but bubbles were absent was very narrow. Only in this range could the bed be operated as a continuous plug flow reactor.

Littman (1964) also compared the solids mixing rates for dense particles ($-140 +200$ mesh copper) in straight and tapered fluidized beds of rectangular cross-section. Gas velocities upto 110% above the MFV and bed

height to diameter ratios of 8 and 16 to 1 were employed. Again it was noted that at gas velocities close to MFV axial solids mixing rates is quite slow.

2.2 LIQUID FLUIDIZATION OF SOLIDS:

Like gas-solid system, here also the point of incipient fluidization is not as clear cut as in cylindrical vessels, as noted by Farkas (1973)¹⁴. It is also noted the point at which pressure drop reaches to a maximum value, just before the sharp decrease is reproducible and so it is selected arbitrarily as the point of incipient fluidization.

Various correlations for the determination of the point of incipient fluidization in tapered vessels have been proposed. The first is due to Galperin et. al (1960)⁸ with basic assumption that bed will start to expand at the flow rate at which the velocity at the top of the bed based on empty cross-section reaches the value of incipient fluidization velocity characteristic of the particular particle fluid system in cylindrical vessels. The same assumption is quoted by Gorshtein and Mukhlcnov (1964)¹⁵. Baskakov and Gal perin (1965)¹⁶ assumed that the bed begins to expand at the moment when the resistance to the flow becomes equal to the net weight of the particles in the container which is

$$W_{\text{nog}} = M = \frac{M}{\rho_s} \quad (3)$$

Here M being the particles weight, ρ_s particle density in the bed, and they gave the correlation,

$$W_{\text{nog}} = \pi \sin^2 \frac{\alpha}{2} \left[C_1 A R_0^2 (R - R_0) U_0 + C_2 B \left(\frac{R_0^2}{R} \right) (R - R_0) U_0^2 \right] \quad (4)$$

The values of C_1 and C_2 are again as given by Ergun (1952) i.e. $C_1 = 150$ and $C_2 = 1.75$ and A and B are as follows:

$$A = \left(\frac{M}{\rho_c \rho_p} \right) (1 - \epsilon)^2 / \epsilon^3$$

$$B = \left(\frac{\rho_f}{\rho_c \rho_p} \right) (1 - \epsilon) / \epsilon^3$$

It should be noted that assumption of Baskakov is quite different from that of Gol'perin et al.⁸ except in case of cylindrical vessels. Recent experimental study made by Farkas (1973)¹⁴ has shown the later as correct. Equation of Baskakov already given can be used to get incipient fluidization velocity from maximum experimental pressure drop value if appropriate values of constants C_1 , C_2 and ϵ are used.

The behaviour of beds composed of particles of mixed size has been investigated in cylindrical beds by McCune and Wilhelm (1949)¹⁹. They observed that the smaller

which relates the resistance of the fixed bed and the fluid velocity:

$$\Delta P = K w_f^2 H_{sta} \rho_{sta} \quad (6)$$

H_{sta} and ρ_{sta} are the height and bulk density of the stationary bed respectively and w_f is superficial fluid velocity at the base.

Another theoretical equation as derived by Gol'povin et al (1960)¹⁵, again valid for laminar flow is, for fixed bed pressure drops

$$\Delta P = K U D (D/D_0 - 1)^2 \tan \alpha/2 \quad (7)$$

The coefficient K is as given:

$$K = C \mu / 2 D_p^D \quad (8)$$

The value of constant C was not given by the authors. Baskakov and Gal'povin (1969)¹⁶ presented the following equation:

$$\Delta P = C_1 A \frac{R}{R_0} (H - R_0) U_0 + C_2 B \left(\frac{R}{3R_0} \right) (H - R_0) U_0^2$$

The Coefficient C_1 and C_2 are the proposed values of Ergun i. e. $C_1 = 150$ and $C_2 = 1.75$, constants A and B have already been described.

Actually the assumption for uniform distribution of gas is far from fulfilled in practice. For this purpose they proposed⁸.

$$\Delta\pi = F (D/D_0, \tan \alpha/2) \quad (10)$$

- true for a single gas solid system, for example for sand-air system the correlation is as given:

$$\Delta\pi_{\text{Expt}} = 2.53 \left(\frac{D}{D_0} \right)^{2.25} (\tan \alpha/2)^{-1.19} \quad (11)$$

Here, ranges of α and D/D_0 are $10-16^\circ$ and $(1 - 30)$ to 6.77 respectively.

In usual practice the ratio $(\Delta\pi/\Delta P)_{\text{Expt}}$ value is lower than theoretical one due to non-uniform distribution of gas which led to the fluidization of a more or less narrow column of material before the mean velocity at the exit cross-section reaches the critical value w_{1-s} i.e. at smaller hydrodynamic resistances of the fluidized bed.

The recent experimental studies made by Farkas (1973)¹⁴ has revealed that conical or tapered vessel data can be correlated by equation of Baskakov if new values of coefficients C_1 and C_2 were substituted for the cylindrical vessel coefficients, even where the apex angle is small. They substituted axial distance Z for radial distance R and $\Phi_S D_p$ for D_p , thus introducing a particle shape factor. Constant C_1 and C_2 are strongly dependent on the geometry of the bed (conical, half conical or two-dimensional), may be due to that the flow distribution

in the packed bed is certainly influenced by the bed form and is most probably not the same as in cylindrical beds. As pointed out by Farkas the pr. drop as to be used above is ΔP_f , frictional losses in the bed and is given by the relation,

$$\Delta P_f = \Delta P_{\text{Gross}} - \Delta P_{\text{Static}} \quad (11)$$

i. e. subtracting from the Gross value the 'static head value' for the bed. This fact can be verified from Bernoulli's equation.

2.4 BED EXPANSION IN TAPERED BEDS:

Kolar (1963)¹⁷ studied expansion of solids particles fluidized with liquid in 10, 20 and 30° conical beds. He correlated average bed porosity with the expressions,

$$\epsilon = 1.037 (U/U_t)^{0.234} \text{ for } 10^\circ \text{ cone and} \quad (12)$$

$$\epsilon = 1.07 (U/U_t)^{0.182} \text{ for } 20^\circ \text{ cone.} \quad (13)$$

In these equations, properties of particles are accounted only through terminal velocity U_t .

Richardson and Zaki (1954)¹⁸ has suggested that more general correlating equation for expansion of liquid fluidized beds in conical/tapered vessel would be:

$$\epsilon^x = U/U_t \quad (14)$$

Here exponent x is expected to depend on particle properties.

Expansion studies by Farkas (1973)¹⁴ have verified the above equation on log-log plot with \bar{U} as ordinate and ϵ as abscissa, the intercept as found is $\log_{10} U_t$ as predicted by this equation, except for 16-18 mesh particles in 5° two-dimensional bed. Here wall effect is considerable and intercept is $\log_{10} U_t - D_p/1.25$ where 1.25 is the spacing between the walls in cm. It is concluded that exponent x depend both on the bed form and on the properties of particles. At larger apex angle particles properties have a smaller influence.

2.5 DESIGN OF TAPERED BEDS:

Levey et. al (1960)¹ observed that in a deep non-tapered bed the upper part was fluidized violently while the lower part was hardly moving at all. By overtapering he was able to obtain a bed in which the lower part was well fluidized while the top of the bed was stationary. In both these cases, there is no true MFV for the bed as a whole.

As the aim is to produce uniform fluidization, the voidage and bed density can be taken uniform thus to keep the gas velocity ~~can be taken uniform thus to keep the gas velocity~~ constant, through out the bed, pressure will be linear function of the bed height above the base.

This based on the assumptions that (i) absolute gas pressure varies linearly with height in a tapered bed (ii) the bed particles are round, smooth and of uniform size (iii) the particles are uniformly packed through out the bed i. e. ϵ is constant, the maintenance of constant gas velocity through out the depth of the bed requires that the cross-sectional area at any point along the axis be inversely proportional to the gas pressure at this point. This led to the following relation,

$$v^2 = \frac{v_b^2}{1 - \frac{\Delta P}{P_b} \frac{L}{L_{mf}}} = \frac{v_t^2}{1 + \frac{\Delta P}{P_t} \frac{L_{mf} - L}{L_{mf}}} \quad (15)$$

where ΔP is given by the relation,

$$\Delta P = L_{mf} P_s (1 - \epsilon_{mf}) = P_b - P_t \quad (16)$$

If pressure drop across an incipiently fluidized bed is equal to the bed weight per unit cross-sectional area, or finally,

$$v^2 = \frac{v_b^2 [P_t + L_{mf} P_s (1 - \epsilon_{mf})]}{P_t + P_s (1 - \epsilon_{mf}) (L_{mf} - L)} \quad (17)$$

$$= \frac{v_t^2 P_t}{P_t + P_s (1 - \epsilon_{mf}) (L_{mf} - L)} \quad (18)$$

Here r is the radius of tapered tube at a axial distance L from the base.

Thus the curvature of the profile being parabolic and this is true for dense materials like copper shot ($\rho_s = 8.93$) but for light materials like sand or glass, the curvature of profile can be ignored and taper is given by the following simplified form:

$$r_t = r_b \sqrt{1 + \frac{L_{mf} \rho_s (1 - \epsilon_{mf})}{P_t}} \quad (18)$$

Actually in cases where bed expansion increases regularly up the bed in proportional to the gas expansion, the tapering is not desirable. It is probable that all beds will exhibit some increased expansion, so that a bed tapered on the assumption of uniform expansion would then be slightly over-tapered. In fact the design formulae as given by Levey et. al (1960)¹. (Eq. 2) give the angle of taper less than the theoretical.

Ridgway (1965)⁶ has concluded that when the pressure drop across the bed is large in compared to absolute gas pressure, effect of gas density along with the velocity change is also to be accounted, because the drag force of the particles is as given by²²,

$$F = C_d \left(\frac{\pi D^2}{4} \right) \rho_f U^2 \quad \text{where } C_d \text{ is drag coeff. (19)}$$

Hence design of taper is to be such that not U^2 but ρU^2 should be constant so that the drag force is constant on the particles which gives the final relation,

$$\gamma^4 = \gamma_b^4 / \left(1 - \frac{\Delta P}{P_b} \frac{l}{l_{mf}} \right) \quad (2)$$

Previous studies carried out by various research workers on fluidization in tapered vessels are confined upto 60° cone angles. Present work involves the study of liquid fluidization in tapered vessels with tapering ranging from 10° to 120°. Coarse size solid particles both spherical and crushed (glass beads, quartz and calcite) in different sizes are used to see the effect of particle size, shape factor, solid density and bed weight/height on pressure peak, pressure drop and liquid flow rate at onset of fluidization.

3. EXPERIMENTAL SETUP AND PROCEDURE :

3.1 EXPERIMENTAL SET UP:

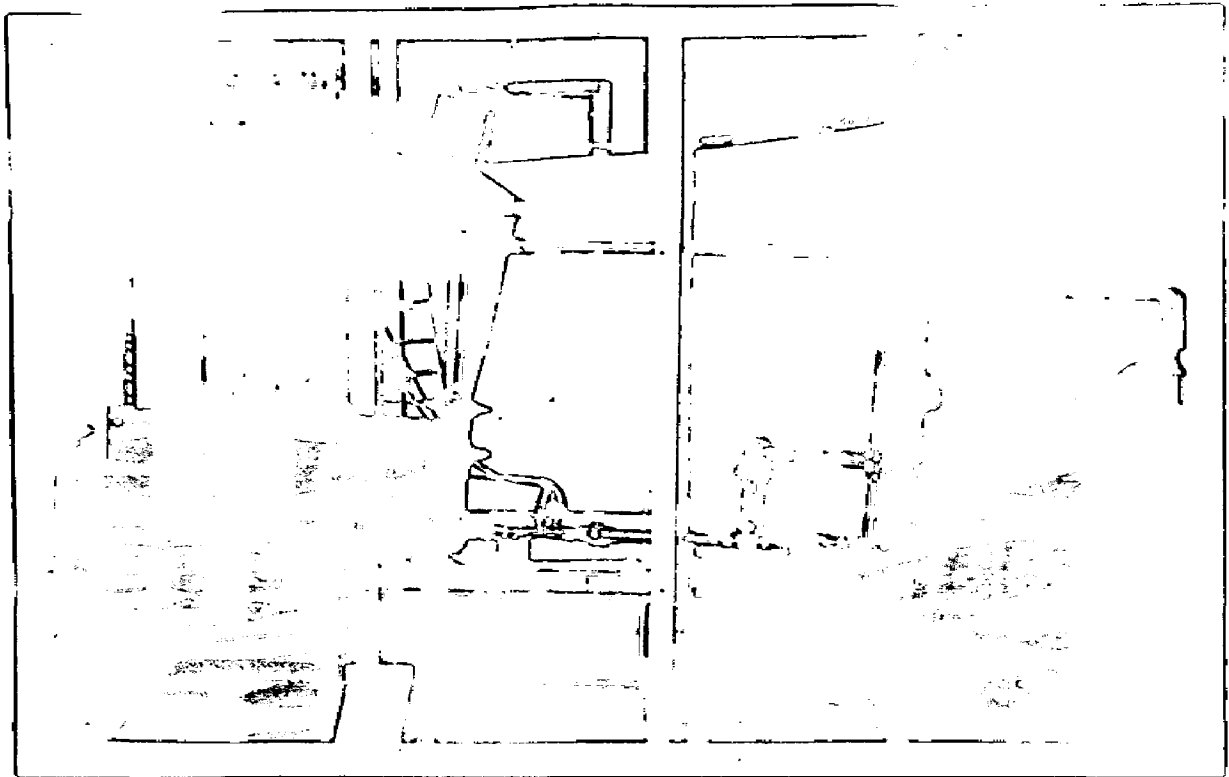
Schematic diagram of the experimental set up is shown in Fig. 3.1 and also in plate No. 1 (a, b).

Set up consists of a tank (1) connected to the inlet of a centrifugal pump (6). Outlet of the pump is connected to the bottom of the fluidizing column (13) through rotameter (7) and venturimeter (9). Rotameter (7) is put in parallel to the main stream line from the pump. Globe valves (A, B and C) are provided to control the liquid flow rates. Overflow from the fluidizing column is delivered back to the tank itself. A grid plate (14) is provided at the bottom of the fluidizing column (13) to support the solid particles. A calming section (12) is also provided below the grid plate packed with 0.5 cm dia. glass beads to smoothen the liquid stream entering to the fluidizing column.

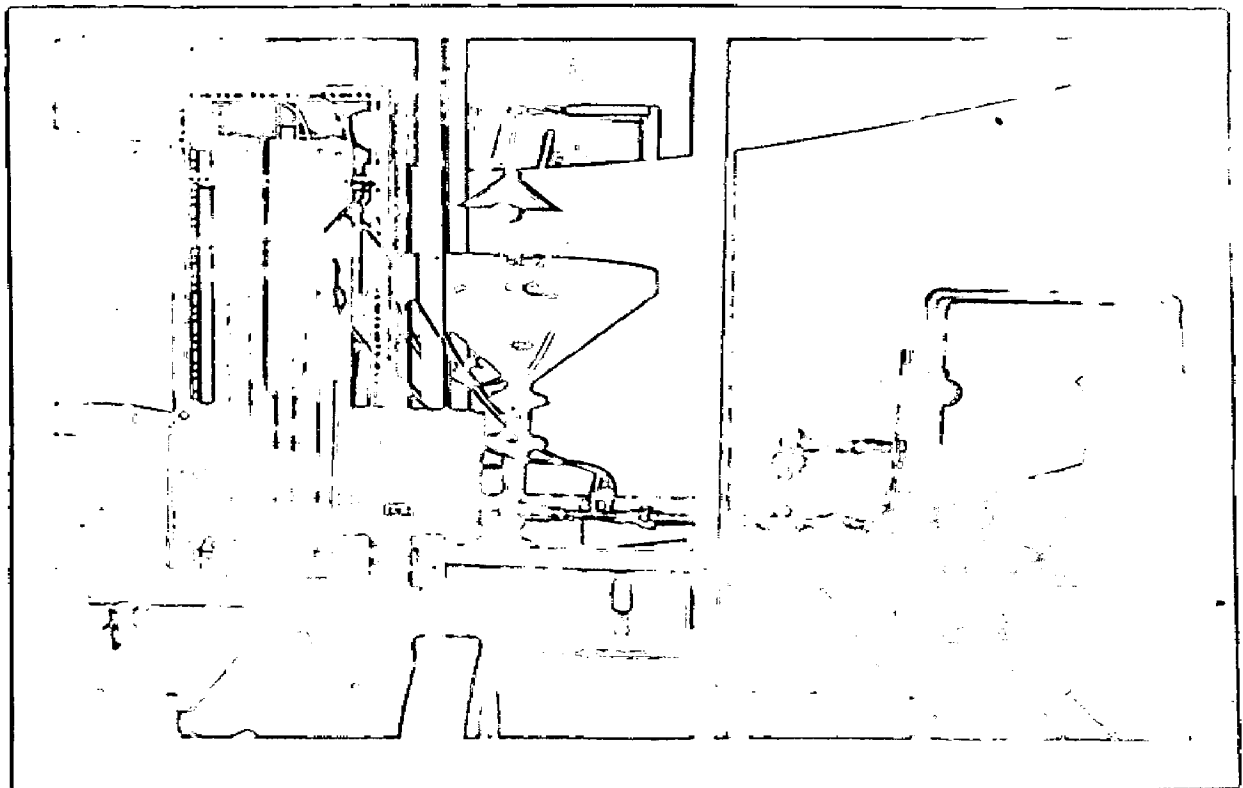
A one meter long carbon tetra chloride-manometer (15) is provided to measure pressure drop across the bed and a 1/2 meter long mercury-manometer (10) across the venturimeter. 3.1(a) fluidizing columns (tapered vessels)

3.1(a) Fluidizing columns (tapered vessels):

Seven different conical vessels with different cone angles i.e. 10° , 15° , 20° , 30° , 45° , 90° and 120°



(A) 20° CONE



(B) 30° CONE

has been used. They are fabricated from 1/16 inch thick mild steel sheet. Bottom diameter of each cone is kept 4 cm. About 12 cms below from the top 1 inch socket is welded for liquid outlet. A 10 cm flange is welded at the bottom of each cone. Through out the height of each cone along the wall, a perspex sheet, 1 inch in width and 1/10 inch thick is fixed by oraldite. Pressure taps are provided at different but equal heights along the wall of each cone.

Detailed drawing of 15° tapered vessel is shown in Fig. 3.2 and for others plate no. 2(a, b) can be followed. Main dimensions of each cone are given in table 3.1.

Table 3.1

Cone angle	Top diameter cm	Bottom diameter cm	Column height cm
10°	12.5	4	50
15°	16.5	4	50
20°	20.0	4	50
30°	22.0	4	50
45°	27.5	4	50
60°	39.5	4	28
120°	62.0	4	17

3.1(b) Grid plate :

Grid plate is made from a 10 cm diameter, 1/32 inch thick aluminium plate. Holes of size $\frac{1}{16}$ in. are

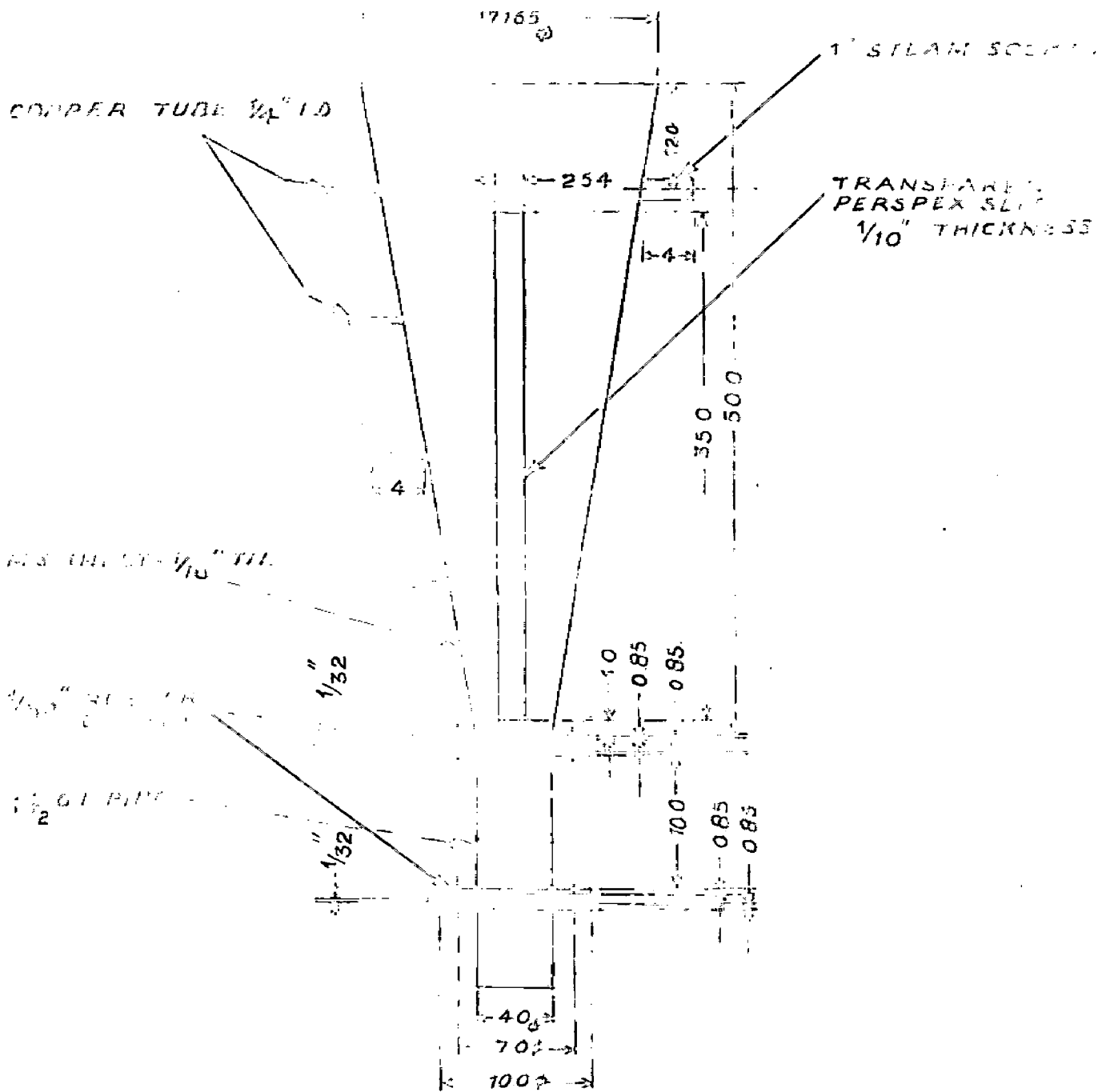
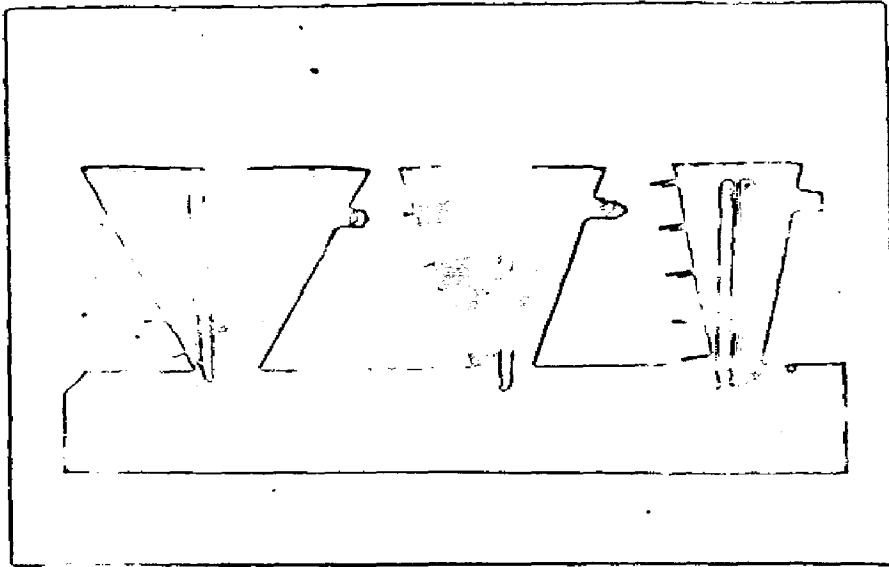
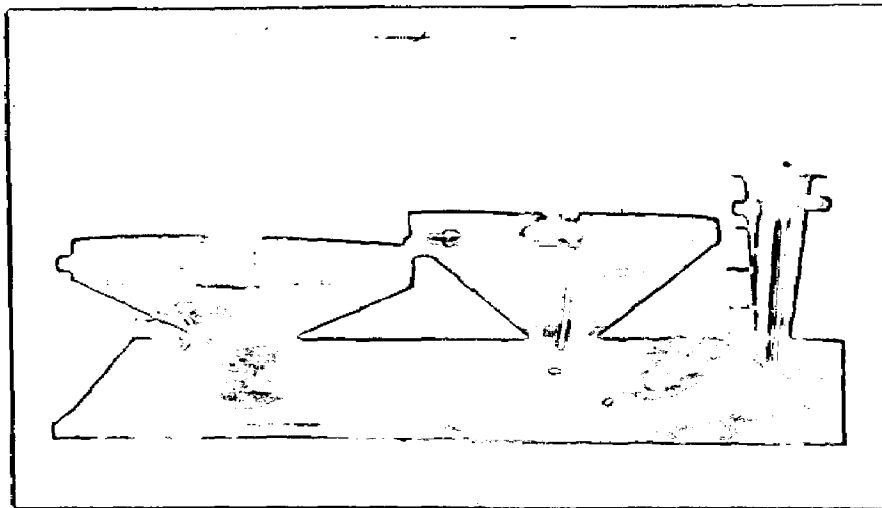


FIG. 1. DESIGN OF FLUIDIZING COLUMN.
 ALL DIMENSIONS IN CM.



45° 30° 20°



120° 90° 10°

PLATE 2. TAPERED VESSELS

drilled in a square pitch of 0.25 cms through out the central portion of the plate in 4.5 cm dia. A fine mesh copper wire cloth piece in 5 cm dia is fixed at the above surface of the plate by araldite.

The same type of plate, except with copper wire mesh is used at the bottom of the calming section so as to support packing material.

3.1(e) Calming Section :

Calming section is made from a 1.5 inch nominal size G.I. pipe of 10 cm long threaded on both sides to have flanges. 0.5 cm dia glass beads are employed as packing material.

3.2 EXPERIMENTAL PROCEDURE :

Data have been taken for three different materials (Glass beads, Quartz and Calcite) in the size range of -8+10, -10+12 and -16+18 mesh nos. (for glass beads instead of -8+10, Mesh size 5 is used). Pressure drop variations and onset of fluidization studies are made for three different bed weights for each sample in steps.

At the start of a run, the weighted amount of material is put in the fluidizing column and initial bed height is noted down. There after pump is started keeping valves 'A' and 'B' closed except 'C' fully open. Now by

gradual opening of valve 'B' flow rate is allowed to increase in gradual steps and corresponding pressure drop across the bed and bed height is noted down. In case when more liquid rate is required beyond the range of rotameter, valve 'A' is allowed to open gradually and pressure drop across venturimeter gives the corresponding liquid flow rate. Care was taken at the limit of stability when pressure drop reaches a maximum value and there after suddenly falls down to a constant value. Thus pressure peak and pressure drop at the onset of fluidization across the bed is noted down. Flow rates are further increased till the whole bed is fully fluidized and particles are under vigorous stirring action.

The data in the same way are repeated for other bed heights and solid materials.

CHAPTER IV

4. EXPERIMENTAL DATA,
RESULT AND DISCUSSION :

The experimental data were obtained in different tapered vessels in fixed bed region and at onset of fluidization. The pressure drop - flow rate data are shown in tables 4.1, 2, 3, 9, 10, 11, 17, 18, 19, 26, 28, 31 and 34 and figures 4.1, 2, 3, 4, 9, 12, 14, 17, 19, 22, 25 and 26 for glass beads, tables 4.4, 5, 6, 12, 13, 14, 20, 21, 22, 26, 29, 32 and 35 and figures 4.5, 6, 7, 8, 10, 13, 15, 18, 20 and 23 for quartz and tables 4.7, 8, 15, 16, 23, 24, 27, 30, 33, 36 and figure 4.11, 16, 21, 24 for calcite.

Effect of bed height :

For the same material and particle size, pressure peak, pressure drop and liquid flow rate at onset of fluidization has been found to increase with bed height/weight.

Higher value of pressure drop is due to more resistance offered by increased no. of particles to liquid flow through the void spaces. Higher value of pressure peak and liquid flow rate is due to increased degree of interlocking between the adjacent particles. So that particles may loose contact with each other and thus may fluidize, a greater liquid force is required. After attaining the pressure peak value, pressure drop suddenly falls down to a steady value corresponding to the net weight of the bed.

Effect of particle size :

For the same material and bed weight, pressure peak value seems to increase with particle size. In addition it is found that there is an intermediate range of particle size for which this value is maximum. Hence it can be concluded that upto particle size 10-12 mesh pressure peak value goes on increasing and when the particle size exceeds this value pressure peak starts falling.

Like pressure peak, liquid flow rate at onset of fluidization is also found to increase with particle size while the pressure drop value at onset of fluidization is almost constant.

Increased value of pressure peak and liquid flow rate is due to increased degree of interlocking between particles as particle size increases while the pressure drop value is almost constant equal to the net weight of the bed. Interlocking is supposed to be more perfect for particle size for which pressure peak is found maximum.

Effect of shape factor :

Pressure peak is found ~~more susceptible~~ to increase as particles are non-spherical in nature. For the same ~~weight~~ pressure peaks for quartz

and calcite are quite high as compared to glass beads. Liquid flow rate at onset of fluidization is a little higher for crushed materials while pressure drop value a little lower, as compared to spherical particles of the same size.

The lower value of pressure drop after the onset of fluidization is due to particles, being completely loose with each other at onset of fluidization, have oriented themselves so as to provide maximum permissible area for flow which is even greater than for spherical particles of the same size.

The higher value of pressure peak and flow rate required at onset of fluidization is due to the non-spherical nature of the particles which have the better interlocking characteristics with each other.

EFFECT OF CONE ANGLE:

For the same material, particle size and bed weight, the values of pressure peak, pressure drop and liquid flow rate at onset of the fluidization decrease as cone angle increases. The reason being that bed height goes on reducing very rapidly with cone angle for the same weight of the bed.

Pressure peak values are noted to be much reduced for 90° cone and even further for 120°. The reason being that (a) the bed heights are quite small in these vessels for the same weight of the bed as in the others (b)

only a limited part of the bed, confined to the central region only is fluidized (see plate no. 36a,b). The solids in between the wall and outside this central region, which consist a major part of the bed, are quite stationary just like as in fixed bed.

Quality of fluidization in different vessels :

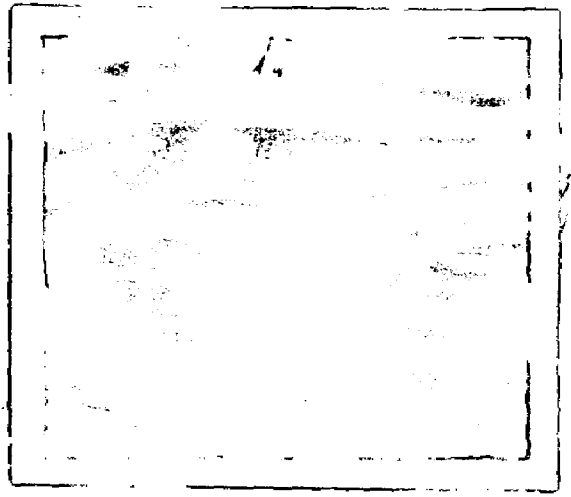
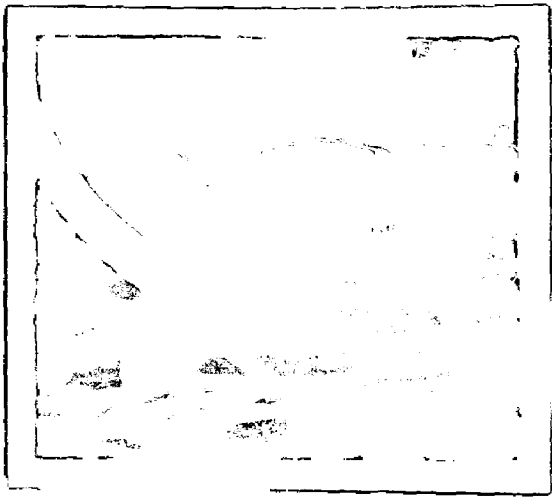
True fluidization is seen to occur in lower cone angles i.e. 10° , 15° , and 20° . In 30° and 45° cones fluidization is just like as in spouted beds, solids may be seen coming down by the side of the wall of vessels and rising up in the central part of the bed upto some height thus having interface at the top of the bed convex instead of being flat as in lower angles. In over tapered beds like 60° and 120° fluidization of solids is only confined to the central region of the bed, leaving the surroundings quite stationary. Even at much higher velocities the same is seen to happen except solids in the central zone go upto much higher distance. It is concluded that all the liquid seems to pass through this central region of the bed.

Actually when angle is less solids have tendency to slide down along the wall so mixing of solids is confined to the whole bed (see Fig. 4.27). The counter-current motion of solids is more pronounced in 30° and 45° cones. In case of over tapered beds since the

angle of cone has increased to such a value, below angle of repose of solid particles that solids have lost the tendency to slide down along the wall hence mixing of solid does not extend to the whole bed (see Fig. 4.28).

As far as fluidization in 10° , 15° and 20° cone angles is concerned it is seen that in 10° cone, glass beads are fluidized in a quite smooth way having clear interface at the top. No slugging inside the bed is seen at all. For both calcite and quartz in this cone, it is seen that whole bed is lifted up upto some distance, compacted, till this starts disintegrating to individual particles and finally to re-formation of the compacted bed which is again lifted up.

As cone angle increases from 10 to 15° slugging goes on reducing for both calcite and quartz. Now whole bed has stopped to be compacted and horizontal water ripples are seen within the bed rising upto some heights and then disappearing themselves. In 20° cone, fluidization for these materials is quite smooth and uniform with clear interface at the top and no slugging inside the bed. For glass beads in these vessels fluidization has worsened. Thus it is concluded that as particles are non-spherical in nature the cone angle required to fluidize them, in a uniform and smooth way is as larger.



(A) 0 0 0 0

(B) 0 0 0 0

PLATE 3. MIXING OF SOILS

IN CENTRAL REGION

BED POROSITY AND PRESSURE DROP AT ONSET OF FLUIDIZATION

It has been observed that for ir-regular particles i.e. Quartz and Calcite bed height goes on reducing with increase in liquid flow rate, till the minimum value is reached at the limit of stability. This is due to reorientation of particles and due to bed compaction effect. Any how the reduction in bed height is very small and almost absent for spherical ones. At onset of fluidization suddenly bed expands a little and goes on expanding as liquid flow rate increases.

Equation 1 has been checked with experimental data and it has been confirmed that it is so not ρ_{avg} in the equation. In table 4.37, ΔP_{Theo} value has been compared with ΔP_{Obs} values for each cone. Mesh size, as selected, is -10+12 and bed weight 1 kg. ΔP_{Obs} is the observed value

Table No. 4.37

Material	$\Delta P_{Theo} = \frac{W_{net}}{a_0}$	ΔP_{Obs}						
		10°	15°	20°	30°	45°	90°	120°
Glass beads	47.6	49.7	43.8	37.7	24.1	14.7	7.2	3.3
Quartz	50.0	46.0	37.6	35.6	30.0	11.8	5.1	3.0
Calcite	50.0	49.5	40.3	33.0	22.2	12.3	6.8	3.3

of pressure drop in gm/cm² (pressure drop, as obtained, is multiplied by 1.595, the sp. gr of C-Cl₄) ΔP_{Theo} is calculated by dividing W_{net} value (eq. 3) with a_0 , area of the cone at the base. Data show that whole bed is suspended in the rising fluid stream at MFV provided the cone angle is low

Table No. 4.1

Cone angle, 10° $D_p = 0.335 \text{ cm}$
 Material, Glass beads $\rho_s = 2.5 \text{ gm/cc}$
 Mesh No., 5 $\phi_s = 1$

Sl. No.	Bcd wt. kg	Liq. flow rate, lit/min.	Manometer legs readings cm		$\Delta P, \text{cm-CC}$	L_c	Bcd ht. cm.
1	0.4	1.8	52.1	2.9	2.9		14.1
2		4.0	55.7	10.2	10.2		14.1
3		6.8	61.7	22.2	22.2*		14.1
4		8.0	65.2	29.2	29.2*		14.1
5		8.0	59.7	10.2	13.2*		16.0
6		12.0	59.5	17.0	17.0		16.0
7		16.0	59.5	17.8	17.8		17.0
<hr/>							
1	0.7	1.4	51.9	49.2	2.7		10.8
2		4.0	59.0	42.2	16.8		10.8
3		7.0	60.8	32.3	30.5		10.8
4		10.0	71.1	27.0	47.1*		10.8
5		10.0	63.3	37.8	26.5*		22.0
6		14.0	63.0	38.0	26.0		22.3
7		18.0	62.8	38.2	24.6		22.8
<hr/>							
1	1.0	1.4	52.0	49.2	2.8		24.4
2		3.9	57.2	43.9	13.3		24.4
3		7.0	63.1	33.0	35.1		24.4
4		11.6	64.1	17.0	67.1*		24.4
5		11.6	66.0	35.1	30.9*		25.7
6		17.6	65.5	35.5	30.0		37.3

* Pressure peak value (at limit of stability) for fixed bed.

x Pressure drop value at onset of fluidization.

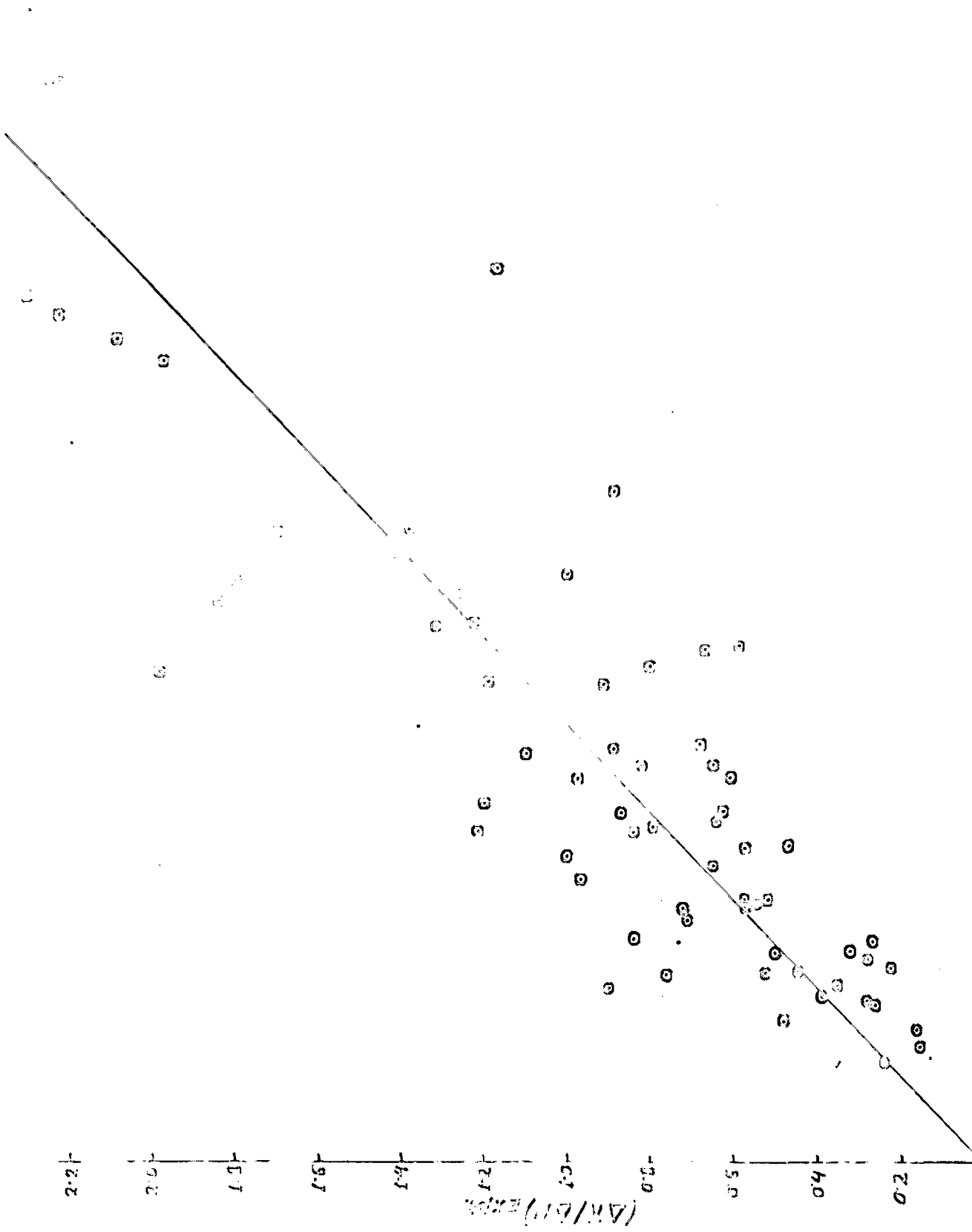


Table No. 4.2

Cone angle, 10°

$D_p = 0.1517 \text{ cm}$

Material, Glass beads

$\rho_s = 2.5 \text{ gm/cc}$

Mesh No., -10+12

$\phi_s = 1$

Sl. NO.	Bed wt. kg	Liq. flow rate, lit/min.	Manometer legs readings, cms		$\Delta P, \text{cm-CCl}_4$	Bed ht. cm
1	0.4	0.7	51.2	47.4	3.8	13.3
2		1.2	52.6	45.9	6.7	13.3
3		2.0	55.8	42.7	13.1	13.3
4		2.7	60.8	37.8	23.0	13.3
5		4.5	65.6	33.0	32.6 [†]	13.3
6		4.5	58.3	40.2	18.1 ^x	14.7
7		6.1	53.1	40.4	17.7	15.0
8		9.0	53.2	40.5	17.5	16.0
<hr/>						
1	0.7	0.0	51.8	46.6	5.2	13.7
2		1.6	55.0	43.4	11.6	13.7
3		2.6	61.0	37.4	23.6	13.7
4		3.5	63.0	30.3	37.7 [†]	13.7
5		5.0	72.8	25.5	47.3 [†]	13.7
6		5.0	61.3	36.7	25.1 ^x	19.3
7		7.4	61.5	36.9	24.6	20.5
8		12.0	61.4	37.0	24.4	22.0
<hr/>						
1		1.1	54.1	46.9	7.2	23.1
2		2.3	64.3	36.6	27.7	23.1
3		3.7	71.3	28.9	42.9	23.1
4		6.0	84.2	16.5	67.7 [†]	23.1
5		6.0	66.0	34.8	31.2 ^x	24.4
6		11.0	65.4	35.4	30.0	25.5

† Pressure peak value (at limit of stability) for fixed bed.

x Pressure drop value at onset of fluidization.

Table No. 4.3

Cone angle, 10° $D_p = 0.0927$ cm
 Material, Glass beads $\rho_s = 2.5$ gm/cc
 Mesh No., -16+18 $\phi_0 = 1$

Sl. No.	Bed wt. kg.	Liq. flow rate, lit/min.	Manometer logs readings, cms.	ΔP , cm- CCl_4	Bed ht. cm	
1		0.7	53.7	46.6	7.1	13.2
2		1.1	56.9	43.4	13.5	13.2
3		1.2	60.5	39.8	20.7*	13.2
4	0.4	2.7	68.3	36.0	32.3*	13.2
5		2.7	59.0	41.4	17.6 ^x	14.1
6		3.9	58.7	41.7	17.0	14.7
7		6.0	58.6	41.9	16.7	15.6
1		0.7	54.5	46.1	8.4	13.7
2		1.1	58.5	42.1	16.4	13.7
3		1.7	63.5	37.1	26.4*	13.7
4	0.7	3.1	72.9	27.7	45.2*	13.7
5		3.1	63.0	37.5	25.5 ^x	20.2
6		6.2	62.6	37.8	24.8	21.0
7		9.0	62.4	38.0	24.4	22.6
1		0.6	56.4	45.1	10.3	22.0
2		1.2	61.8	38.8	23.0*	22.0
3	1.0	3.8	84.4	16.0	68.4*	22.0
4		3.8	65.8	34.7	31.1 ^x	24.8
5		5.8	66.9	35.4	30.6	26.0

* Pressure peak value (at limit of stability) for fixed bed.

x Pressure drop value at onset of fluidization.

107926

INDIAN INSTITUTE OF TECHNOLOGY
ROORKEE

Table No. 4.4

Conc angle, 10°

$D_p = 0.1865 \text{ cm}$

Material, quartz

$\rho_0 = 2.7 \text{ gm/cc}$

Mesh No., 20-10

$\phi_0 =$

Sl. No.	Bed wt. kg.	Liq. flow rate, lit/min.	Manometer readings cms.	legs	$\Delta P, \text{cm-CCl}_4$	Bed ht. cm.
1		0.3	51.3	49.3	2.0	14.7
2		2.0	53.5	40.9	6.6	14.6
3		3.2	57.8	42.8	15.0	14.6
4		4.0	62.8	37.8	25.0	14.6
5	0.4	4.4	67.1	33.5	33.5 _y	14.6
6		6.7	80.2	20.3	60.0 _y	18.1
7		6.7	58.8	41.7	17.1 _x	10.0
8		11.6	53.5	42.0	10.5	17.6
9		16.5	58.2	42.2	16.0	10.0
1		0.3	51.6	49.0	2.5	20.0
2		2.1	54.4	46.1	8.3	20.0
3		3.0	59.6	41.0	18.6	20.6
4		4.0	66.7	34.0	32.7	20.5
5	0.7	9.2	85.6	15.0	70.6 _y	20.5
6		9.2	62.0	38.5	23.5 _x	22.4
7		12.4	61.5	39.0	22.5	22.5
8		10.5	61.2	39.2	22.0	24.5
1		0.6	51.4	49.2	2.2	25.4
2		2.9	57.2	43.4	13.8	25.4
3		4.5	65.8	34.9	30.9	25.3
4	1.0	6.0	75.3	25.3	50.0 _y	25.2
5		10.4	99.1	1.5	97.6 _x	25.2
6		10.4	65.0	36.0	29.0 _x	27.0
7		14.0	63.8	36.8	27.0	27.8

◇ Pressure peak value (at limit of stability) for fixed bed.

x Pressure drop value at onset of fluidization.

Table No. 4.6

Cone angle, 10°

$$D_p = 0.1517 \text{ cm}$$

Material, Quartz

$$\rho_s = 2.7 \text{ gm/cc}$$

Mesh No., 10-12

$$\phi_s =$$

Sl. No.	Bed wt. kg.	Liq. flow rate, lit/min.	Manometer logs readings, cm.	$\Delta P, \text{cm-CCl}_4$	Bed ht. cm.	
1		1.2	55.0	45.9	9.1	13.7
2		2.2	60.6	40.2	20.4*	13.6
3	0.4	5.2	74.5	26.6	48.0*	13.5
4		5.2	58.7	42.0	16.7 ^x	16.2
5		7.7	58.6	42.2	16.3	17.0
6		10.4	58.4	42.3	16.1	18.5
1		0.7	52.7	48.2	4.5	20.3
2		2.4	62.1	39.0	23.1	20.0
3	0.7	3.6	71.0	30.0	41.0*	20.0
4		6.6	80.0	11.0	79.0*	19.7
5		6.6	62.4	38.8	23.6 ^x	22.6
6		9.6	61.0	39.5	22.5	23.2
1		0.7	52.6	48.7	3.9	25.4
2		1.7	57.2	44.1	13.1	25.2
3		2.9	66.7	38.7	30.0	24.9
4	1.0	4.4	81.2	19.5	61.7*	24.7
5		7.3	80.0	20.0	96.0*	24.7
6		7.3	64.8	36.0	28.8 ^x	26.7
7		9.2	66.6	36.3	23.3	27.6
8		11.2	63.7	37.0	26.7	28.5

* Pressure peak value (at limit of stability) for fixed bed.

x Pressure drop value at onset of fluidization.

Table No. 4.6

Cone angle, 10°

$$\sigma_p = 0.0027 \text{ cm}$$

Material, Quartz

$$\rho_s = 2.7 \text{ gm/cc}$$

Mesh No., 10-18

$$\phi_s =$$

Sl. No.	Bed wt. kg.	Liq. flow rate, lit/min.	Monometer readings, cms.	Monometer legs	$\Delta P, \text{cm-CCl}_4$	Bed ht. cm.
1		1.0	54.6	46.3	8.3	15.3
2		1.7	59.5	41.5	18.0 ⁺	15.3
3	0.4	4.0	68.8	32.2	36.6 ⁺	15.2
4		4.0	58.9	42.2	16.7 ⁺	17.4
5		4.9	58.7	42.3	16.4	18.0
6		7.2	58.6	42.4	16.2	19.5
1		0.8	55.0	46.0	0.0	21.4
2		1.7	62.7	38.5	24.2	21.3
3		2.4	69.5	31.8	37.7 ⁺	21.1
4	0.7	4.6	85.2	15.8	69.4 ⁺	21.1
5		4.6	62.2	38.9	23.3 ⁺	23.7
6		6.5	62.8	39.6	23.2	24.0
7		9.0	61.7	39.4	22.3	25.0
1		0.8	55.4	45.7	0.7	26.3
2		2.1	66.4	34.9	31.5	26.2
3		2.8	74.0	27.3	46.7	26.1
4	1.0	3.4	81.5	19.5	62.0 ⁺	26.1
5		4.9	90.0	11.0	79.0 ⁺	26.1
6		4.9	65.2	35.8	29.4 ⁺	28.7
7		6.4	64.4	36.7	27.7	29.0
8		10.0	64.0	37.2	26.8	30.0

* Pressure peak value (at limit of stability) for fixed bed.

π Pressure drop value at onset of fluidization.

Table No. 4.7

Cono angle, 10° $D_p = 0.1865 \text{ cm}$
 Material, Calcite $\rho_s = 2.7 \text{ gm/cc}$
 Mesh No., -8+10 $\phi_s =$

Sl. no.	Bod wt. kg	Liq. flow rate, lit/min.	Manometer readings cms	legs	$\Delta P, \text{cm-CCl}_4$	Bod ht. cm
1		1.1	52.0	48.8	3.2	14.0
2		1.8	53.9	47.1	6.8	13.8
3		3.0	59.0	42.1	16.9	13.6
4		4.5	67.5	33.5	34.0	13.5
5	0.4	6.6	71.5	29.5	42.0 [†]	13.5
6		6.6	59.9	40.9	19.0 [‡]	15.7
7		3.0	59.5	41.3	18.2	16.6
8		11.4	50.3	41.6	17.7	17.3
<hr/>						
1		1.1	52.2	48.5	3.7	20.0
2		2.6	56.8	44.1	12.7	19.3
3		3.3	63.4	37.5	25.9	19.7
4	0.7	5.0	74.5	26.5	48.0	19.7
5		10.3	34.3	16.3	63.0 [†]	19.7
6		10.0	63.2	37.7	25.5 [‡]	22.3
7		14.0	62.7	38.0	24.7	22.3
<hr/>						
1		0.9	52.5	48.8	3.7	24.3
2		2.7	59.4	42.1	17.3	24.1
3		3.9	67.9	33.6	34.3	23.0
4		5.2	73.9	22.3	56.6	24.0
5		9.6	96.5	3.5	63.0 [†]	24.0
6		9.6	66.1	34.7	31.4 [‡]	20.4
7		12.0	65.5	35.5	30.0	27.2
8		15.0	65.0	36.0	29.0	23.0

† Pressure peak value (at limit of stability) for fixed bed.

‡ Pressure drop value at onset of fluidization.

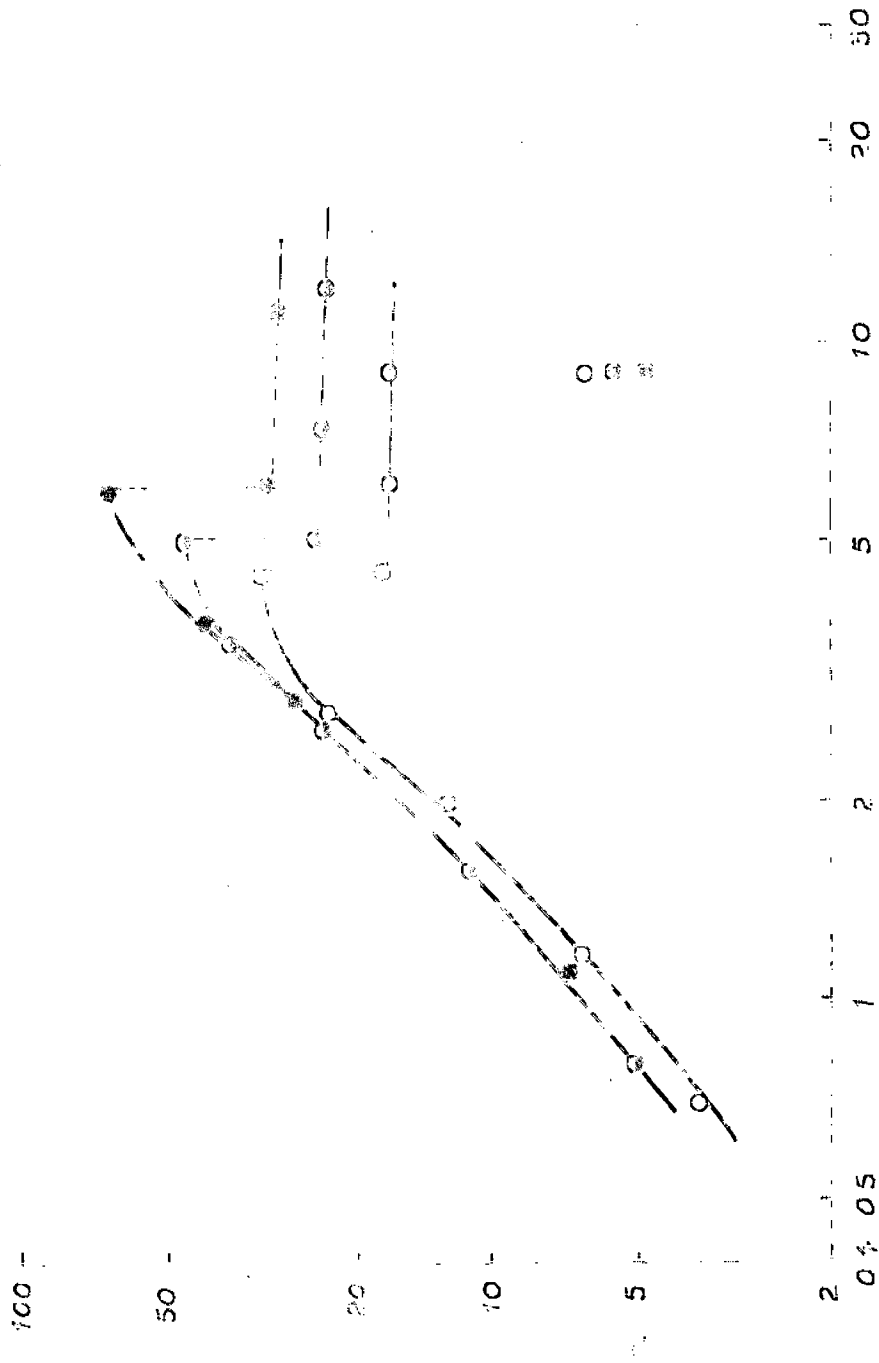
Table No. 4.8

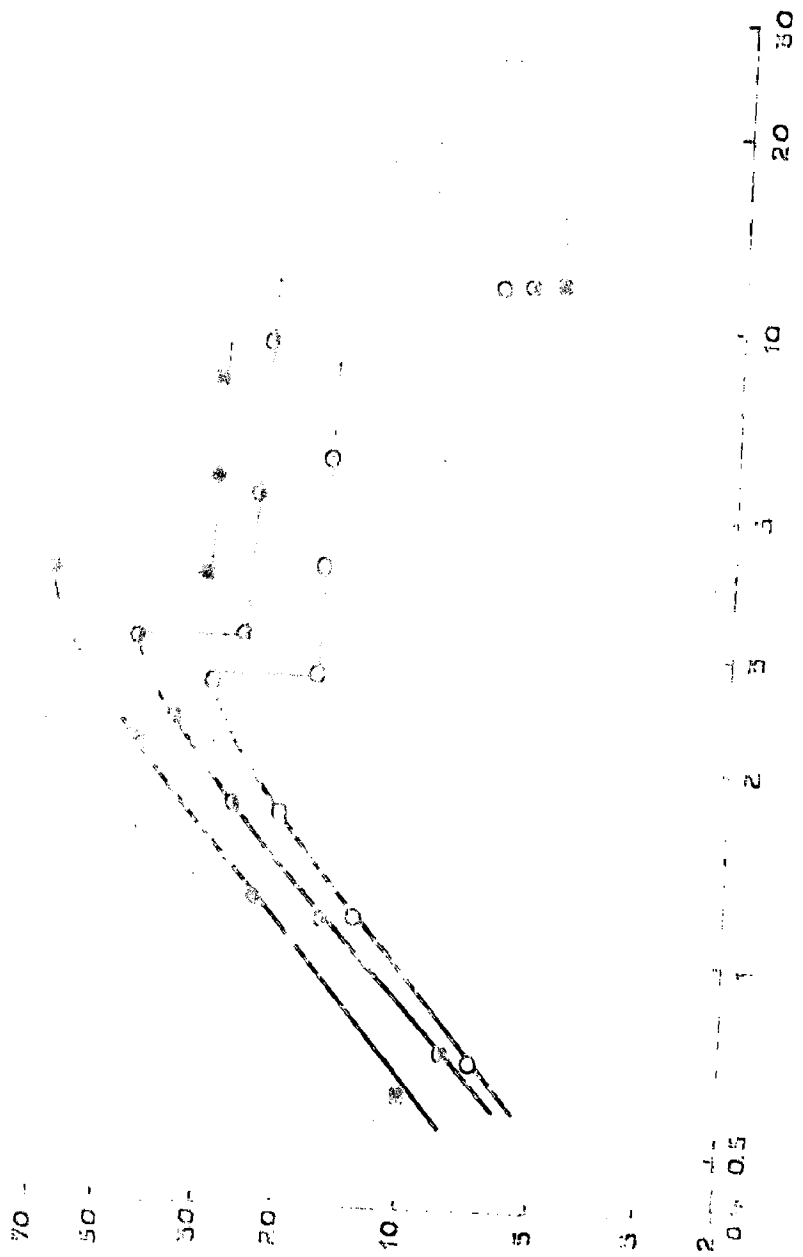
Cone angle, 10° $D_p = 0.1517 \text{ cm}$
 Material, Calcite $\rho_s = 2.7 \text{ gm/cc}$
 Mesh No., -10+12 $\phi_0 =$

Sl. No.	Bed wt. kg	Liq. flow rate, lit/min.	Manometer legs readings, cm	$\Delta P, \text{cm-CCl}_4$	Bed ht. cm	
1	0.4	1.0	52.8	47.3	5.0	14.0
2		1.7	56.2	44.5	11.7	13.3
3		2.3	61.0	39.7	21.3	13.5
4		3.1	66.0	34.5	31.5*	13.5
5		5.0	71.6	29.0	42.0*	13.6
6		6.3	69.2	41.5	17.7 ^x	16.0
7		7.2	58.9	41.7	17.2	16.0
8		10.0	53.3	41.9	16.9	17.6
<hr/>						
1.	0.7	0.7	52.7	48.1	4.6	10.0
2		1.7	57.8	43.0	14.8	13.7
3		3.0	68.5	32.5	36.0	19.5
4		3.6	72.6	28.4	44.1*	19.6
5		7.4	89.8		73.8*	16.5
6		7.4	62.7	38.3	24.4 ^x	22.3
7		10.0	62.4	38.6	23.8	23.0
8		12.0	62.0	39.0	23.0	23.7
<hr/>						
1.	1.0	0.0	53.3	47.7	5.6	24.0
2		1.7	58.2	42.9	15.3	24.6
3		3.2	70.3	30.9	39.4	24.4
4		3.9	73.8	22.2	56.6*	24.3
5		6.4	100.6	-0.5	100.0*	24.3
6		6.4	65.9	34.9	31.0 ^x	26.6
7		9.0	65.2	35.5	29.7	27.2
8		12.0	64.4	36.3	23.1	25.0

* Pressure peak value (at limit of stability) for fixed bed.

x Pressure drop value at onset of fluidization.







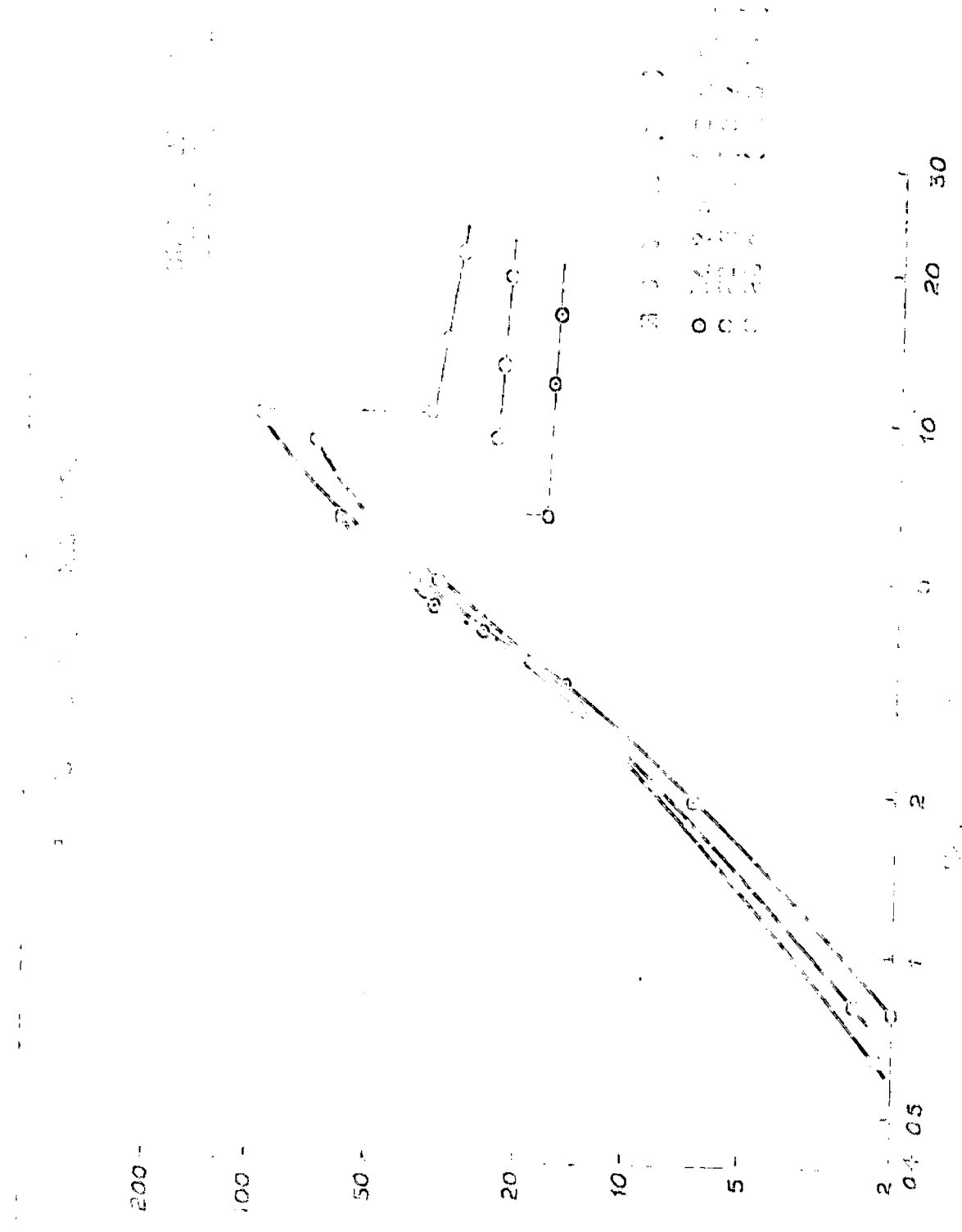
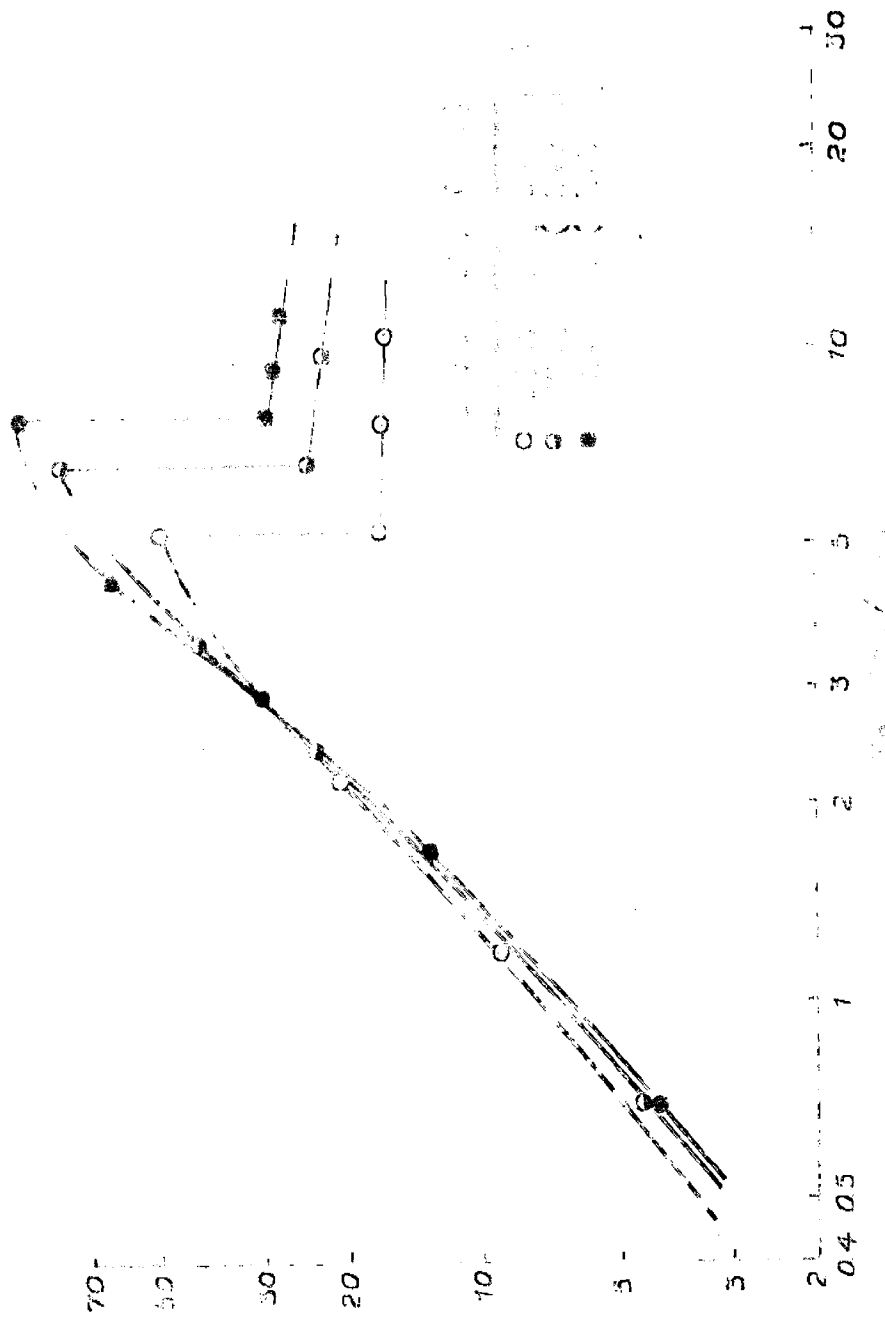


Figure 1. Plot of $\log_{10}(\text{Y-axis})$ versus X-axis . The symbols represent different experimental conditions or parameters as defined in the legend.



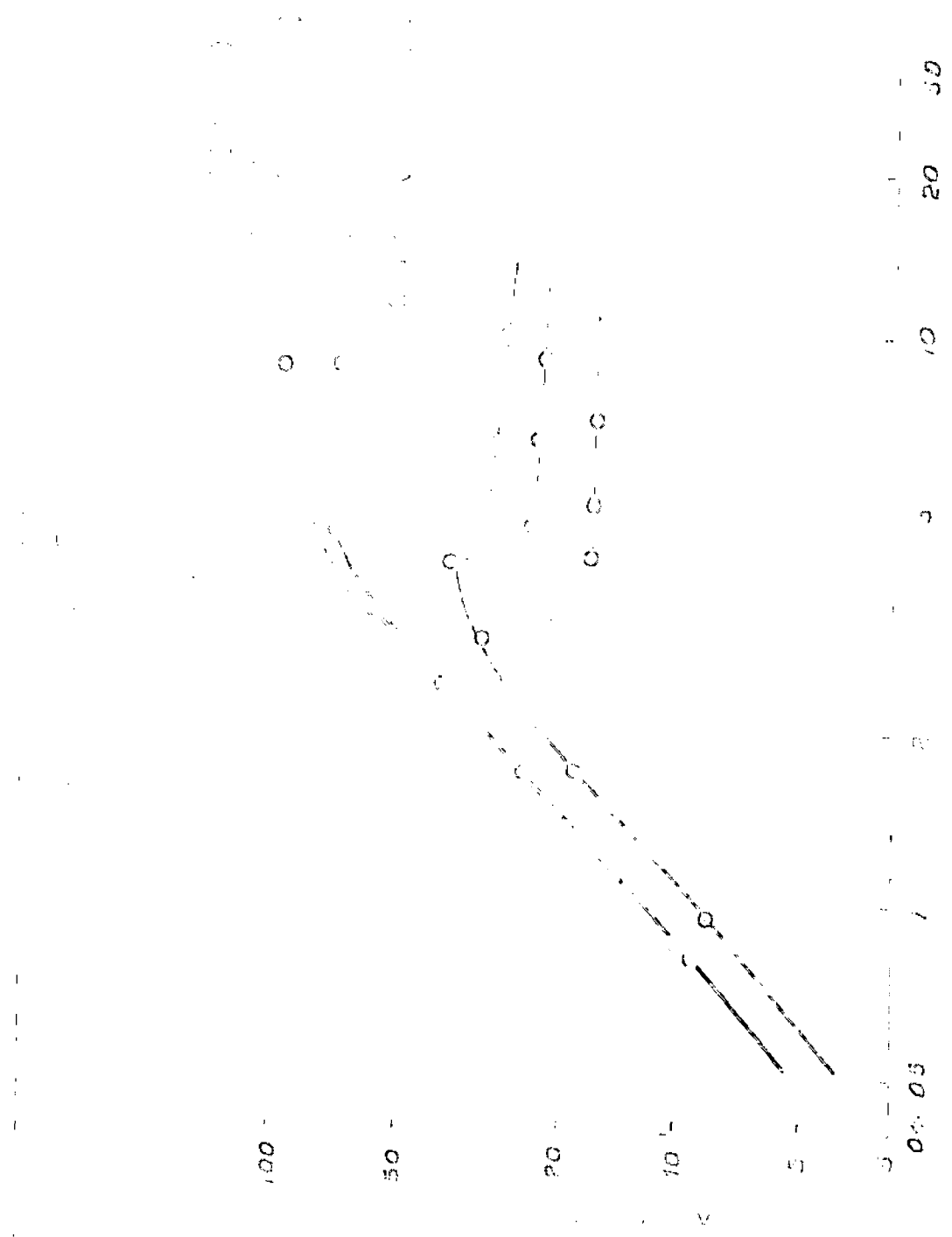




Table No. 4.9

Cone angle, 15°

$$D_p = 0.335 \text{ cm}$$

Material, Glass beads

$$\rho_s = 2.5 \text{ gm/cc}$$

Mesh No., 5

$$\phi_s = 1$$

Sl. No.	Bed wt. kg.	Liq. flow rate, lit/min.	Manometer readings cm.		ΔP , gm- CCl_4	Bed ht. cm.
1		1.3	60.3	48.1	2.2	11.1
2		2.4	51.1	47.2	3.9	11.1
3		3.9	53.7	44.7	9.0	11.1
4	0.4	4.4	55.7	42.7	13.0	11.0
5		6.9	59.1	39.3	19.8*	11.0
6		6.9	56.7	41.6	15.1 ^x	11.0
7		9.6	56.6	41.9	14.6	12.0
1		1.1	60.2	48.0	2.2	10.1
2		2.7	52.1	46.2	5.9	10.1
3		3.8	54.8	43.8	11.3	16.1
4		5.4	59.9	38.6	21.4*	16.1
5	0.7	7.6	66.0	33.4	31.6*	16.0
6		7.8	60.9	38.5	21.4 ^x	16.6
7		11.6	59.4	39.0	20.4	17.8
8		13.5	59.1	39.2	19.9	18.8
1		1.2	50.4	47.9	2.5	19.8
2		2.7	52.3	46.9	6.4	19.0
3		4.0	55.4	42.8	12.6	19.8
4		6.1	62.0	36.3	26.7*	19.8
5	1.0	10.1	71.6	26.7	44.9*	19.8
6		10.0	62.0	36.2	25.8 ^x	20.7
7		14.0	61.5	36.7	24.8	21.5
8		17.5	61.3	36.8	24.5	22.4

* Pressure peak (at limit of stability) for fixed bed.

^x Pressure drop at onset of fluidization.

Table No. 4.10

Conc angle, 16°

$D_p = 0.1517 \text{ cm}$

Material, Glass Beads

$\rho_s = 2.5 \text{ gm/cc}$

Mesh No., 10+12

$\phi_s = 1$

Sl. No.	Bed wt. kg.	Liq flow rate lit/min.	Manometer readings cm.	$\Delta P, \text{cm-CCl}_4$	Bed ht. cm.	
1	0.4	0.7	51.3	47.3	4.0	10.9
2		0.9	52.0	46.6	5.4	10.9
3		1.3	53.5	46.1	8.4	10.9
4		1.9	56.5	42.0	14.5 ⁺	10.9
5		2.8	59.5	39.0	20.5 ⁺	10.9
6		2.8	57.4	41.1	16.3 ^x	11.4
7		3.6	57.2	41.3	15.9	11.0
8		5.2	57.0	41.5	15.5	12.1
9		7.0	56.9	41.6	15.3	12.6
1	0.7	0.6	51.5	46.8	4.7	16.0
2		0.9	52.6	45.8	6.8	15.0
3		1.7	56.8	41.6	15.2	15.7
4		2.2	60.8	37.8	23.0 ⁺	15.6
5		3.5	67.4	33.5	36.2 ⁺	15.6
6		3.5	60.5	38.0	22.5 ^x	16.1
7		4.4	60.3	38.1	22.2	16.8
8		6.8	59.8	38.6	21.2	17.0
9		10.0	59.8	38.0	21.2	18.0
1	1.0	0.5	51.4	47.1	4.3	19.4
2		1.0	53.7	44.7	9.0	19.3
3		2.0	60.0	38.5	21.5 ⁺	19.1
4		4.2	72.0	26.5	45.5 ⁺	19.0
5		4.2	63.0	35.5	27.5 ^x	19.0
6		6.8	62.5	36.0	26.5	20.3
7		11.4	62.1	36.3	25.8	21.0

† Pressure peak (at limit of stability) for fixed bed.

x Pressure drop at onset of fluidization.

Table No. 4.11

Cone angle, 15°

$D_p = 0.0927 \text{ cm}$

Material, Glass beads

$\rho_s = 2.5 \text{ gm/cc}$

Mesh No., -16+18

$\phi_s = 1$

Sl. No.	Bed wt. kg.	Liq. flow rate, lit/min.	Manometer readings cms.		$\Delta P, \text{cm-CCl}_4$	Bed ht. cm.
1	0.4	0.5	52.7	45.8	6.9	10.9
2		0.7	53.9	44.6	9.3	10.9
3		0.8	54.7	43.9	10.8	10.9
4		0.9	55.2	43.4	11.8	10.9
5		1.6	58.6	40.0	18.6 ⁺	10.9
6		1.6	57.4	41.2	16.2 ^x	11.3
7		1.9	57.3	41.2	16.1	11.5
8		2.4	57.1	41.5	15.6	11.8
9		3.2	57.0	41.7	15.3	12.0
10		5.0	56.8	41.8	15.0	13.0
<hr/>						
1	0.7	0.5	52.2	46.2	6.0	15.9
2		0.7	55.1	43.5	11.6	15.6
3		1.2	60.1	38.5	21.6	15.5
4		2.1	55.9	38.8	39.2 ⁺	15.4
5		2.1	60.2	38.4	21.8 ^x	15.9
6		2.5	60.1	38.4	21.7	16.2
7		3.5	59.7	38.6	21.1	16.6
8		6.2	59.7	38.8	20.9	18.6
<hr/>						
1	1.0	0.4	52.2	46.1	6.1	19.4
2		0.6	54.7	43.7	11.0	18.9
3		1.2	61.3	37.2	24.1	18.7
4		1.4	63.2	35.4	27.8	18.6
5		2.6	69.8	28.5	41.3 ^x	18.6
6		2.6	62.7	36.8	26.9 ^x	19.8
7		4.5	62.2	36.4	25.8	20.1
8		7.0	62.1	36.5	25.6	20.6

+ Pressure peak (at limit of stability) for fixed bed.

x Pressure drop at onset of fluidization.

Table No. 4.12

Cono angle, 15° $D_p = 0.1865$ cm
 Material, Quartz $\rho_s = 2.7$ gm/cc
 Mesh No., -2010 $\phi_D =$

Sl. No.	Bcd wt. kg.	Liq. flow rate, lit/min.	Manometer readings cms.		$\Delta P, \text{cm-CCl}_4$	Bcd ht. cm.
1	0.4	1.0	50.6	48.0	2.6	12.1
2		2.5	54.1	44.5	9.6	11.9
3		4.0	59.0	39.7	19.3 ⁺	11.8
4		6.8	64.2	34.5	29.7 ⁺	11.0
5		6.8	56.7	41.9	14.8 ⁺	12.0
6		9.6	56.3	42.3	14.0	13.0
7		14.0	53.2	42.4	13.8	14.0
<hr/>						
1	0.7	0.3	50.3	48.3	2.0	17.2
2		3.0	56.0	42.0	13.4	16.3
3		4.5	62.1	36.5	25.6 ⁺	16.7
4		8.0	72.6	26.0	46.6 ⁺	16.0
5		8.0	59.3	39.1	20.2 ⁺	18.5
6		12.0	63.8	39.8	19.0	19.0
7		22.0	52.6	39.9	13.7	20.0
<hr/>						
1	1.0	0.8	50.2	48.3	1.9	20.0
2		1.5	51.4	47.2	4.2	20.4
3		3.0	56.0	42.9	13.1	20.3
4		4.0	61.8	37.0	24.8	20.2
5		5.0	70.5	28.4	42.1 ⁺	20.1
6		9.0	61.2	17.7	63.5 ⁺	20.0
7		9.0	62.0	36.6	25.4 ⁺	21.2
8		11.0	61.0	37.5	23.6	22.0
9		22.0	59.9	38.6	21.3	21.5

+ Pressure @ peak (at limit of stability) for fixed bcd.

π Pressure drop at onset of fluidization.

Table No. 4.13

Cone angle, 15°

 $D_p = 0.1617 \text{ cm}$

Material, Quartz

 $\rho_s = 2.7 \text{ gm/cc}$

Mesh No. -10+12

 $\phi_s =$

Sl. No.	Bed wt. kg.	Liq. flow rate, lit/min.	Manometer readings cms.	ΔP , cm- CCl_4	Bed ht. cm.	
1		0.6	61.7	48.4	3.3	19.1
2		1.1	53.9	46.3	7.6	11.9
3		1.6	56.7	43.4	13.3 ⁺	11.8
4	0.4	3.5	68.6	34.5	31.1 ^x	11.8
5		3.5	57.9	42.3	15.7 ^x	12.7
6		7.0	67.3	42.8	14.5	13.0
7		14.0	56.9	43.2	13.7	14.6
1		0.5	61.2	49.0	2.2	17.3
2		1.5	56.2	44.9	10.3	17.0
3		2.6	61.8	38.2	23.6 ⁺	16.9
4		6.0	73.0	22.0	56.0 ⁺	16.3
5	0.7	6.6	60.0	40.0	20.0 ^x	17.9
6		6.0	59.8	40.3	19.5	18.5
7		9.6	59.2	40.8	18.4	19.3
8		14.0	50.1	40.9	18.2	20.0
1		0.5	61.1	48.0	2.3	21.0
2		2.1	57.5	42.5	15.0	20.8
3		3.5	66.2	33.8	32.4	20.7
4	1.0	7.4	86.3	13.7	72.6 ⁺	20.0
5		7.4	61.7	38.1	23.6 ^x	21.5
6		10.6	61.2	38.7	22.5	22.0
7		10.0	60.8	39.2	21.6	23.5

+ Pressure peak (at limit of stability) for fixed bed.

x Pressure drop at onset of fluidization.

Table No. 4.14

Cone angle, 15° $D_p = 0.0927 \text{ cm}$
 Material, Quartz $\rho_s = 2.7 \text{ gm/cc}$
 Mesh No. -16+18 $\phi_s =$

Sl. No.	Bed wt. kg.	Liq. flow rate, lit/min.	Manometer readings cm.	$\Delta P, \text{cm-CCl}_4$	Bed ht. cm.	
1		0.7	53.2	46.6	6.6	12.9
2		1.2	56.7	43.3	13.4 ⁺	12.0
3		2.4	64.0	36.0	28.0 ⁺	12.5
4	0.4	2.4	57.2	42.6	14.6 ^x	13.3
5		3.0	57.0	42.8	14.2	14.4
6		12.0	56.4	43.3	13.1	15.1
1		0.6	52.0	47.5	5.1	17.5
2		1.6	59.6	40.5	19.1 ⁺	17.3
3		3.5	69.4	30.7	38.7 ⁺	17.2
4	0.7	3.5	59.9	40.1	19.8 ^x	19.0
5		6.2	59.8	40.3	19.5	19.5
6		6.6	59.3	40.7	18.6	19.9
7		9.2	59.3	40.8	18.5	20.3
1		0.0	62.9	47.6	5.3	21.5
2		1.5	59.4	42.0	16.4	21.3
3		2.0	62.4	38.0	24.4 ⁺	21.3
4	1.0	4.0	74.9	25.5	49.4 ⁺	21.2
5		4.6	61.7	38.3	23.4 ^x	22.7
6		6.3	61.9	38.6	22.7	23.5
7		8.5	60.8	39.3	21.6	24.3

† Pressure peak (at limit of stability) for fixed bed.

x Pressure drop at onset of fluidization.

Table No. 4.16

Cone angle, 15°

 $D_p = 0.1265 \text{ cm}$

Material, Calcite

 $\rho_s = 2.7 \text{ gm/cc}$

Mesh No. -8+10

 $\phi_s =$

Sl. No.	Bed wt. kg.	Eq. flow rate, lit/min.	Manometer readings, cms.		$\Delta P, \text{ on-CCl}_4$	Bed ht. cm.
1		0.8	50.0	48.2	1.8	12.1
2		2.1	52.3	45.9	16.4	12.1
3		3.4	57.0	41.5	15.5*	12.0
4		6.5	63.8	34.6	29.0*	11.9
5	0.4	6.5	56.8	41.6	15.2**	12.8
6		8.0	56.6	41.7	14.9	13.5
7		10.0	56.1	42.2	13.9	13.9
8		16.0	56.0	42.3	13.7	14.4
1		0.8	50.4	48.2	2.2	10.4
2		1.9	52.8	46.0	6.8	10.2
3		3.4	58.6	40.1	18.5	10.1
4		4.7	64.8	33.8	31.0*	10.1
5	0.7	7.0	73.6	25.0	48.6**	10.0
6		7.0	69.2	33.3	21.9**	17.1
7		9.0	60.7	33.8	26.9	17.0
8		12.4	59.2	39.2	20.0	13.0
9		16.5	53.6	40.0	13.6	10.1
1		0.8	50.0	48.5	1.5	20.3
2		2.6	55.7	42.7	13.0	20.0
3		3.9	62.5	36.0	26.5	20.0
4		5.1	69.4	29.2	40.2*	19.0
5	1.0	10.0	87.6	11.0	76.6**	19.0
6		10.0	61.9	36.5	25.4**	21.8
7		12.0	61.4	37.0	24.4	22.0
8		17.6	60.3	38.1	22.2	22.6
1		1.3	52.1	48.0	4.1	25.1
2		2.0	56.6	43.5	13.0	25.1
3		6.0	66.4	33.7	32.6	25.1
4		7.4	80.5	19.4	61.1	25.0
5	1.5	9.0	92.7	7.2	85.5	24.9
6		13.0	105.0	5.0	110.0*	24.9
7		13.0	65.8	34.2	31.6**	27.1
8		21.0	64.7	35.2	29.5	23.1
9		30.0	64.0	36.0	28.0	30.1

* Pressure peak (at limit of stability) for fixed bed.

** Pressure drop at onset of fluidization.

Table No. 4.16

Cone angle, 15°

$$D_p = 0.1617 \text{ cm}$$

Material, Calcite

$$\rho_s = 2.7 \text{ gm/cc}$$

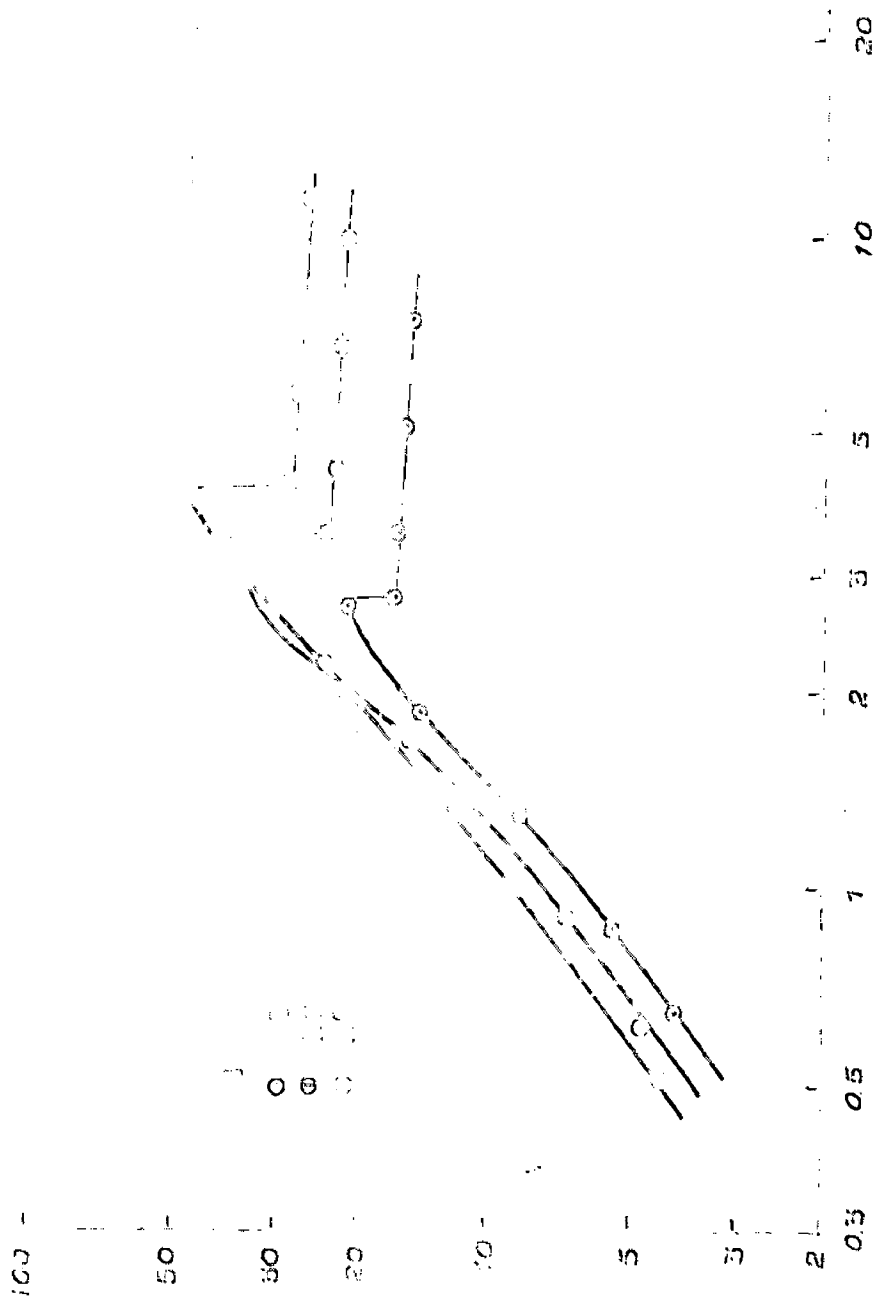
Mesh No. $20+10$

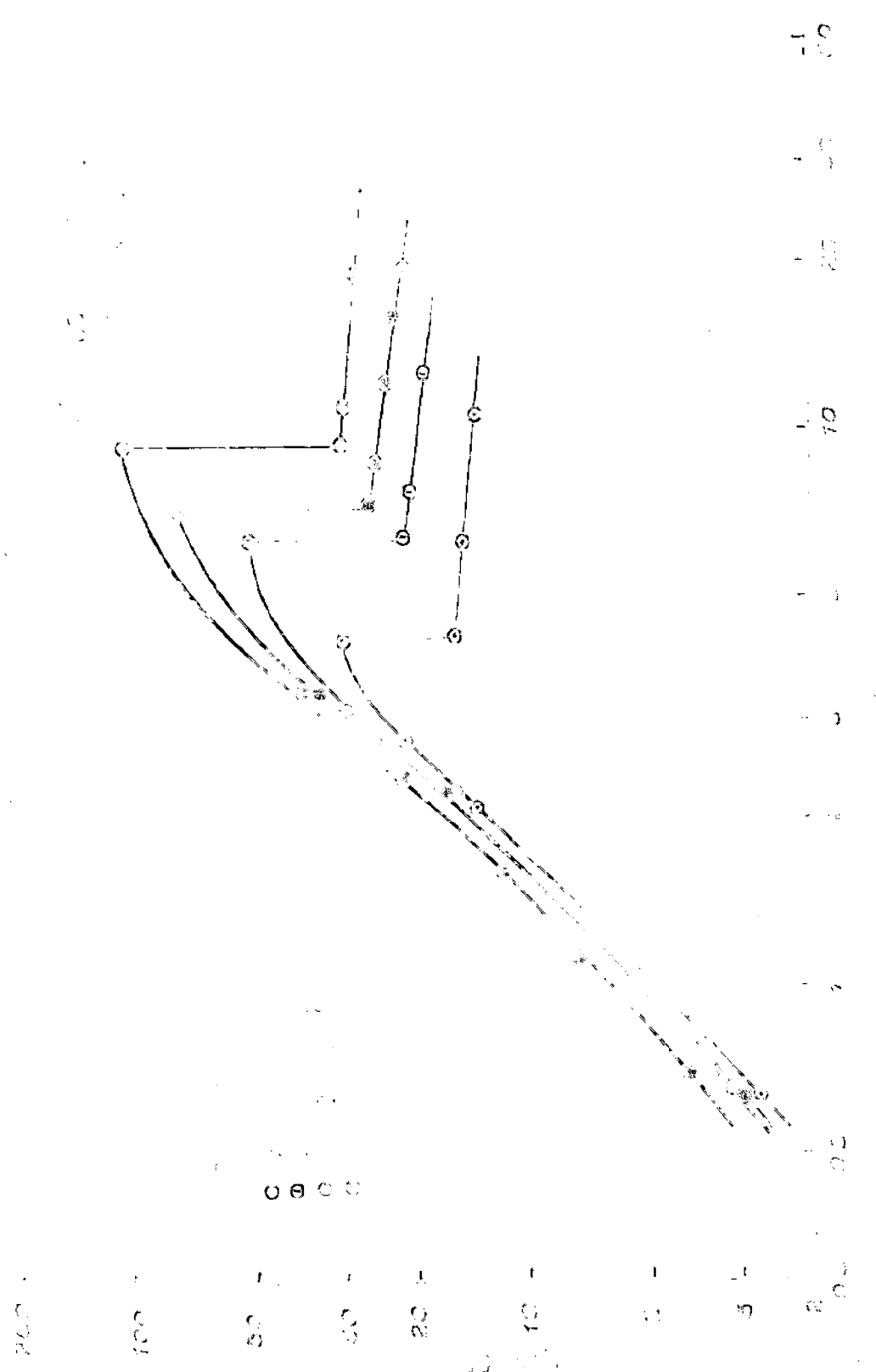
$$\phi_0 =$$

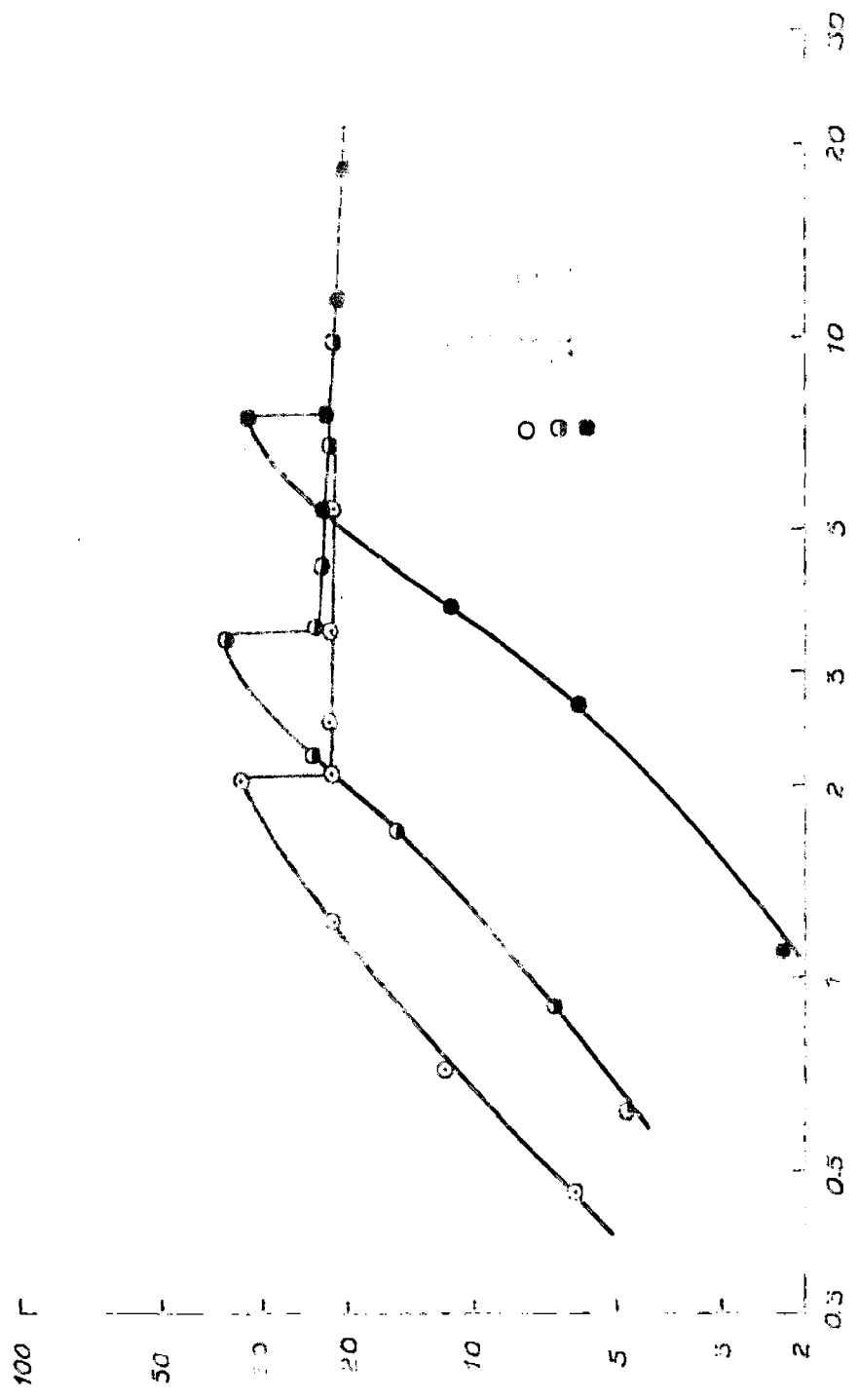
Sl. No.	Bed wt. kg.	Liq. flow rate, lit/min.	Manometer readings cms.		$\Delta P, \text{cm. CCl}_4$	Bed ht. cm.
1	0.4	0.7	50.7	48.0	2.7	11.6
2		2.2	56.2	42.6	3.6	11.5
3		2.8	59.8	39.0	20.8 ⁺	11.5
4		4.4	63.8	34.8	29.0 ⁺	11.4
5		4.4	67.2	41.6	16.7 ^x	12.3
6		6.4	60.7	41.9	18.8	13.5
7		10.2	53.3	42.4	13.9	14.6
1	0.7	0.7	50.9	47.8	3.1	10.8
2		2.3	57.2	41.5	15.7	16.0
3		3.2	63.0	36.1	26.9 ⁺	16.4
4		6.6	74.3	24.6	49.8 ⁺	16.4
5		6.6	59.8	38.8	21.0 ^x	17.7
6		3.0	59.6	39.2	20.3	18.5
7		13.0	53.7	40.0	10.7	19.0
1	1.0	0.6	58.0	55.1	2.9	20.1
2		2.2	64.8	48.2	16.6	20.0
3		3.5	73.7	39.2	34.5 ⁺	19.9
4		7.6	82.9	10.1	74.8 ⁺	19.3
5		7.5	69.1	43.8	25.3 ^x	21.7
6		9.0	68.0	44.3	23.7	22.0
7		12.4	63.3	44.8	23.5	22.5
8		16.4	67.7	45.3	22.4	23.0
9		20.0	67.0	46.0	21.0	23.5
1	1.5	0.7	52.3	48.8	4.0	21.5
2		1.1	64.0	46.5	7.6	21.5
3		1.6	59.0	44.5	11.5	21.4
4		2.4	60.5	39.8	20.7	21.3
5		3.5	68.3	31.9	36.4 ⁺	21.3
6		0.0	100.0	0.0	100.0 ^x	21.3
7		9.0	65.5	34.8	30.7 ^x	27.0
8		11.2	64.7	35.7	29.0	27.5
9		20.0	63.7	36.5	27.2	28.0

⁺ Pressure peak (at limit of stability) for fixed bed.

^x Pressure drop at onset of fluidization.







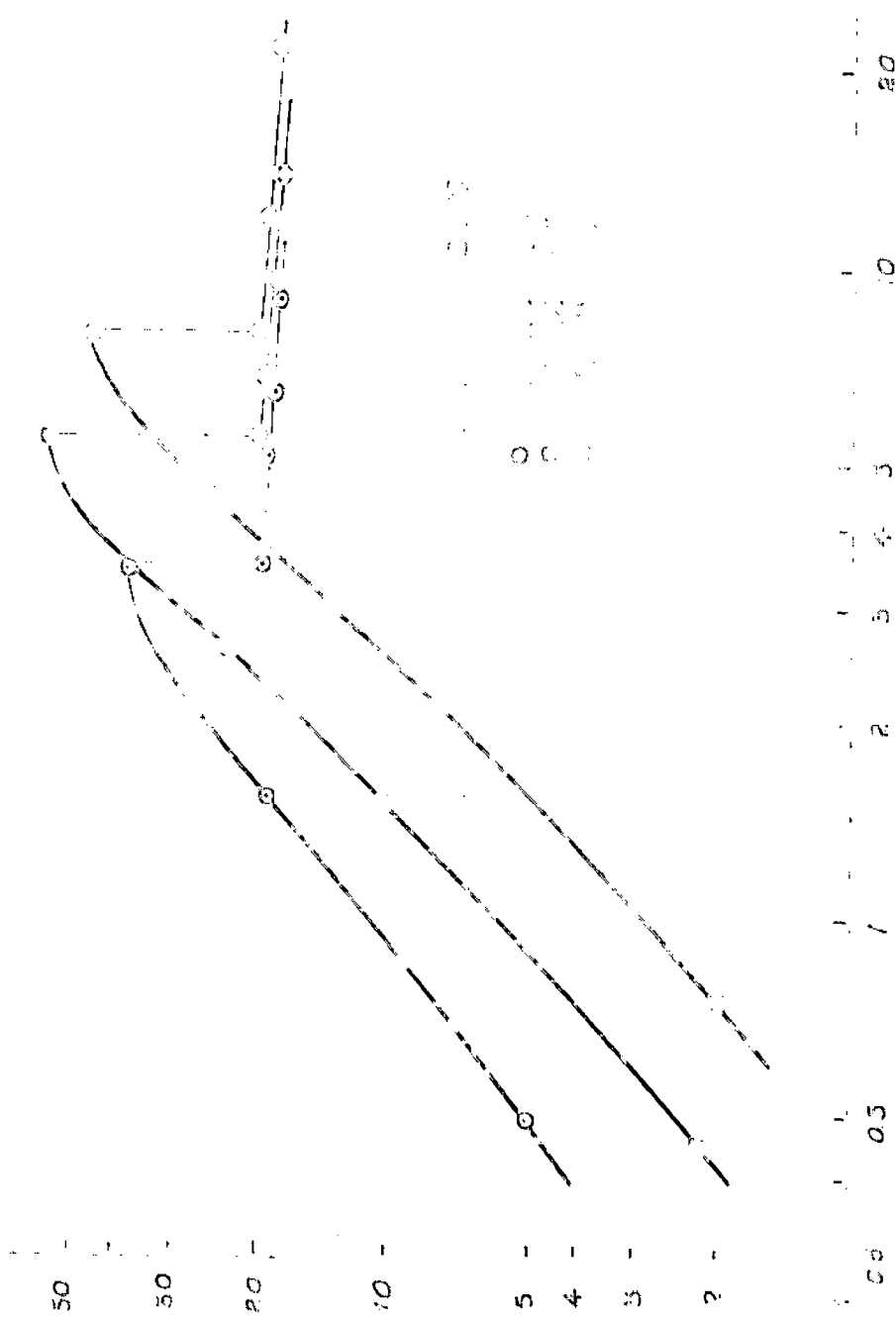


Figure 1. Comparison of the results of the present study with those of other authors.

Table No. 4.17

Conc angle, 20°

$$D_p = 0.236 \text{ cm}$$

Material, Glass beads

$$\rho_s = 2.5 \text{ gm/cc}$$

Mesh No., 5

$$\phi_s = 1$$

Sl. No.	Bed wt. kg.	Liq. flow rate, lit/min.	Manometer readings cm.		$\Delta P, \text{cm-CCl}_4$	Bed ht. cm.
1		1.3	40.0	44.1	1.9	10.0
2		2.2	47.1	43.0	4.1	10.0
3		3.8	49.7	40.4	9.3	10.0
4	0.4	6.0	56.9	33.2	23.7*	10.0
5		6.0	52.0	30.1	13.9 ^x	10.6
6		11.0	51.7	30.4	13.3	11.7
7		19.2	51.0	39.0	12.0	13.3
1		1.4	40.0	41.1	1.9	14.6
2		3.0	47.9	42.3	5.6	14.6
3		4.2	50.1	40.0	10.1	14.6
4	0.7	7.2	58.0	32.0	26.0*	14.6
5		7.2	54.7	35.5	19.2 ^x	14.8
6		11.2	54.4	35.7	18.7	15.6
7		19.0	53.6	36.5	17.1	16.3
1		1.0	40.6	43.6	3.0	17.4
2		3.0	43.5	41.7	0.8	17.4
3		4.8	52.9	37.3	15.6	17.4
4	1.0	5.0	58.2	35.0	20.2*	17.4
5		8.0	60.7	29.5	31.2 ^x	17.4
6		8.0	56.4	33.8	22.6 ^x	17.8
7		14.8	56.0	34.2	21.8	18.7
8		22.4	55.1	35.1	20.0	19.7

* Pressure peak (at limit of stability) for fixed bed.

^x Pressure drop at onset of fluidization.

Cone angle, 20°

$$D_p = 0.1517 \text{ cm}$$

Material, Glass beads

$$\rho_0 = 2.5 \text{ gm/cc}$$

Mesh No., -10+12

$$\phi_0 = 1$$

Sl. No.	Bed wt. kg.	Liq. flow rate, lit/min.	Manometer readings cm.		ΔP_{on-CCl_4}	Bed ht. cm.
1		0.5	45.8	44.1	1.7	10.3
2		1.0	47.4	42.3	5.1	10.3
3		1.7	50.9	38.0	12.9	10.3
4	0.4	2.8	52.9	35.0	18.9 [†]	10.3
5		2.8	52.3	37.6	14.7 [‡]	10.5
6		4.2	52.0	37.7	14.3	10.9
7		6.0	51.3	33.0	18.3	11.3
8		10.0	51.7	33.1	18.6	12.3
<hr/>						
1		0.5	45.8	43.8	2.0	14.5
2		0.9	47.4	42.3	5.1	14.5
3		1.4	50.8	38.9	11.9	14.5
4	0.7	1.9	54.1	35.6	18.5	14.5
5		3.4	59.7	30.0	29.7 [†]	14.5
6		3.4	58.0	34.8	23.2 [‡]	14.8
7		4.0	54.6	35.1	19.5	15.0
8		6.4	54.5	35.3	19.2	15.3
9		11.2	54.3	35.6	18.7	16.3
<hr/>						
1		0.7	47.0	42.8	4.2	17.5
2		1.3	50.2	39.5	10.7	17.5
3		1.7	53.0	36.7	16.3	17.5
4	1.0	2.0	55.5	34.2	21.3 [†]	17.5
5		4.0	64.7	25.0	39.7 [‡]	17.5
6		4.0	53.7	33.1	20.6 [‡]	17.7
7		8.0	53.3	33.4	22.9	18.2
8		12.0	56.0	33.7	22.3	18.7

† Pressure point (at limit of stability) for fixed bed.

‡ Pressure drop at onset of fluidization.

Table No. 4.19

Cone angle, 20°

$$D_p = 0.0027 \text{ cm}$$

Material, Glass beads

$$\rho_s = 2.5 \text{ gm/cc}$$

Mesh No., -16+18

$$\phi_s = 1$$

Sl. No.	Bed wt. kg.	Liq. flow rate, lit/min.	Manometer readings cms.		$\Delta P, \text{cm-CCl}_4$	Bed ht. cm.
1		0.3	46.5	43.5	3.0	10.0
2		0.5	47.6	42.3	5.3	10.0
3		0.9	50.5	39.4	11.1	10.0
4	0.4	1.2	52.4	37.5	14.9 [*]	10.0
5		1.3	54.4	35.5	18.9 [*]	10.0
6		1.8	52.5	37.3	15.2 ^x	10.2
7		2.4	52.4	37.5	14.9	10.3
8		4.0	51.2	37.9	14.0	11.1
1		0.3	46.9	42.9	4.0	14.0
2		0.6	49.0	40.7	8.3	14.0
3		0.8	51.8	38.0	13.8	14.0
4	0.7	1.3	54.6	35.3	19.3 [*]	14.0
5		2.2	57.4	32.5	24.9 [*]	14.0
6		2.2	55.3	34.6	20.7 ^x	14.3
7		3.4	55.0	34.9	20.1	14.9
8		6.4	54.5	35.5	19.0	16.8
1		0.3	47.4	42.4	5.0	16.9
2		0.6	50.2	39.6	10.6	16.9
3		1.0	53.8	36.1	17.7	16.9
4	1.0	1.6	57.4	32.4	25.0 [*]	16.9
5		2.7	61.4	28.5	32.9 [*]	16.9
6		2.7	57.4	32.5	24.9 ^x	17.2
7		4.4	56.9	33.0	23.9	17.7
8		7.6	56.2	33.6	22.6	18.2

* Pressure peak (at limit stability) for fixed bed.

x Pressure drop at onset of fluidization.

Table No. 4.20

Conc angle, 20° $D_p = 0.1865 \text{ cm}$
 Material, Quarts $\rho_s = 2.7 \text{ gm/cc}$
 Mesh No., -8+10 $\phi_s =$

Sl. No.	Bed wt. kg.	Liq. flow rate, lit/min.	Manometer readings cms.		$\Delta P, \text{cm-CCl}_4$	Bed ht. cm.
1		0.8	46.5	44.2	2.1	10.6
2		2.0	49.5	41.1	8.5	10.6
3		2.4	51.0	39.5	11.5	10.4
4	0.4	4.0	55.0	35.5	19.5 [*]	10.4
5		4.0	52.5	38.0	14.5 [†]	10.7
6		6.4	51.9	38.6	13.3	11.0
7		9.6	51.0	39.5	11.5	11.8
<hr/>						
1		1.0	47.3	44.0	3.3	14.6
2		1.7	49.2	41.7	7.5	14.4
3		2.4	52.2	38.5	13.7	14.3
4	0.7	2.7	54.0	37.0	17.0 [*]	14.3
5		5.0	60.5	30.5	30.0 [†]	14.2
6		8.0	55.7	36.2	19.5 [†]	14.8
7		6.5	54.8	36.0	18.8	15.3
8		10.0	54.0	37.0	17.0	15.8
<hr/>						
1		1.0	46.8	43.6	3.2	18.7
2		1.9	50.0	40.5	9.5	18.6
3		3.0	55.0	34.5	20.5 [*]	18.5
4	1.0	6.0	65.5	25.0	40.5 [*]	18.2
5		6.0	55.7	34.7	21.0 [†]	18.7
6		10.0	55.0	35.3	19.7	19.7

* Pressure peak (at limit of stability) for fixed bed.
 † Pressure drop at onset of fluidization.

Table No. 4.21

Cone angle, 20°

$$D_p = 0.1517 \text{ cm}$$

Material, Quartz

$$\rho_s = 2.7 \text{ gm/cc}$$

Mesh No. 10+12

$$\phi_s =$$

Sl. No.	Bed wt. kg.	Liq. flow rate, lit/min.	Manometer readings cms.		$\Delta P, \text{cm-CCl}_4$	Bed ht. cm.
1		0.8	47.1	43.3	3.8	10.8
2		1.7	49.5	41.0	8.5	10.8
3		2.4	52.5	38.0	14.5 [*]	10.7
4	0.4	3.8	55.5	36.0	20.5 [*]	10.6
5		3.8	52.0	38.5	13.5 ^{**}	11.3
6		5.0	51.7	39.0	12.7	11.3
7		7.2	50.7	40.0	10.7	12.3
1		0.8	47.4	42.9	4.5	15.7
2		1.4	49.5	40.8	8.7	15.6
3		2.0	52.5	37.7	14.8	15.5
4	0.7	2.3	54.5	35.8	18.7 [*]	15.5
5		4.4	60.3	30.0	30.3 ^{**}	15.4
6		4.4	54.5	30.0	18.5 ^{**}	10.2
7		6.6	53.6	36.8	16.7	16.7
8		7.6	53.3	37.0	16.3	17.2
1		0.5	46.5	44.0	2.5	18.7
2		1.6	50.0	40.0	10.0	18.6
3		2.6	55.2	36.0	20.2 [*]	18.6
4	1.0	5.0	62.7	27.5	35.2 ^{**}	18.4
5		5.0	56.3	34.0	22.3 ^{**}	19.2
6		6.0	56.0	34.3	21.7	19.7
7		8.0	55.0	35.5	19.5	20.7

* Pressure peak (at limit of stability) for fixed bed.

** Pressure drop at onset of fluidization.

Table No. 4.22

Cone angle, 29°

 $D_p = 0.0927 \text{ cm}$

Material, Quartz

 $\rho_s = 2.7 \text{ gm/cc}$

Mesh No., -16+18

 $\phi_0 =$

Sl. No.	Bed wt. kg.	Liq. flow rate, lit/min.	Manometer Readings cm.	$\Delta P, \text{cm-CCl}_4$	Bed ht. cm.	
1		0.6	47.2	43.1	4.1	11.6
2		1.2	50.0	40.5	9.5	11.5
3		1.6	52.0	38.5	13.5 _*	11.5
4	0.4	2.4	55.3	35.2	20.1 _*	11.4
5		2.4	52.0	38.5	13.5 ^x	11.8
6		3.2	51.5	39.0	12.5	12.3
7		6.2	51.2	39.2	12.0	13.3
1		0.4	46.6	43.8	2.8	10.1
2		1.1	51.0	39.5	11.5	16.0
3		1.6	54.5	36.0	18.5 _*	15.9
4	0.7	2.8	59.0	31.5	27.5 _*	15.7
5		2.8	54.5	36.0	18.5 ^x	16.2
6		3.6	54.0	36.5	17.5	16.7
7		6.2	53.7	37.0	16.7	17.3
8		8.0	53.0	37.5	15.5	18.2
1		0.6	48.0	42.4	5.6	19.4
2		1.1	50.8	39.7	11.1	19.3
3		1.7	55.0	35.5	19.5	19.2
4		2.2	53.0	32.5	25.5 _*	19.2
5	1.0	3.8	62.5	28.0	34.5 _*	19.1
6		3.8	56.1	34.2	21.9 ^x	19.5
7		5.0	55.5	35.0	20.5	20.1
8		7.2	54.9	35.6	19.3	21.0

* Pressure peak (at limit of stability) for fixed bed.

x Pressure drop at onset of fluidization.

Table No. 4-23

Cone angle, 20°

$$D_p = 0.1865 \text{ cm}$$

Material, Calcite

$$\rho_s = 2.7 \text{ gm/cc}$$

Mesh No., 20-10

$$\phi_s =$$

Sl. No.	Bed wt. kg.	Liq flow rate, lit/min.	Manometer readings cms.		$\Delta P, \text{cm-CCl}_4$	Bed ht. cm.
1		0.8	45.9	44.5	1.4	10.6
2		1.3	46.6	43.9	2.7	10.6
3		2.7	49.1	41.4	7.7 [*]	10.6
4		6.0	53.0	32.5	20.5 [*]	10.4
5	0.4	6.0	52.4	33.0	19.4 [*]	11.0
6		7.2	52.2	33.1	19.1	11.6
6		11.2	51.5	33.8	17.7	12.6
8		16.0	50.3	32.8	17.5	13.3
<hr/>						
1		1.1	46.2	44.2	2.0	15.1
2		2.3	48.2	42.2	6.0	15.1
3		3.4	51.4	39.0	12.4	15.0
4		5.0	56.3	33.5	22.8 [*]	14.9
5	0.7	7.3	61.3	25.5	35.8 [*]	14.9
6		7.6	54.0	36.3	17.7 [*]	15.0
7		9.6	53.9	36.3	17.6	15.8
8		13.6	53.2	37.2	16.0	16.8
9		16.0	52.5	37.7	14.8	17.3
<hr/>						
1		1.5	46.9	43.5	3.4	18.4
2		3.0	50.4	40.0	10.4	18.3
3		3.8	53.7	36.5	17.2	18.3
4		4.9	59.0	31.5	27.5	18.2
5	1.0	6.0	63.5	26.5	37.0 [*]	18.1
6		8.6	74.0	16.0	58.0 [*]	18.0
7		8.6	65.3	34.9	30.4 [*]	18.4
8		15.2	64.8	35.6	29.2	20.2

* Pressure peak (at limit of stability) for fixed bed.

x Pressure drop at onset of fluidization.

Table No. 4.24

Cone angle, 20° $D_p = 0.1517 \text{ cm}$
 Material, Calcite $\rho_s = 2.7 \text{ gm/cc}$
 Mesh No., -10+12 $\phi_s =$

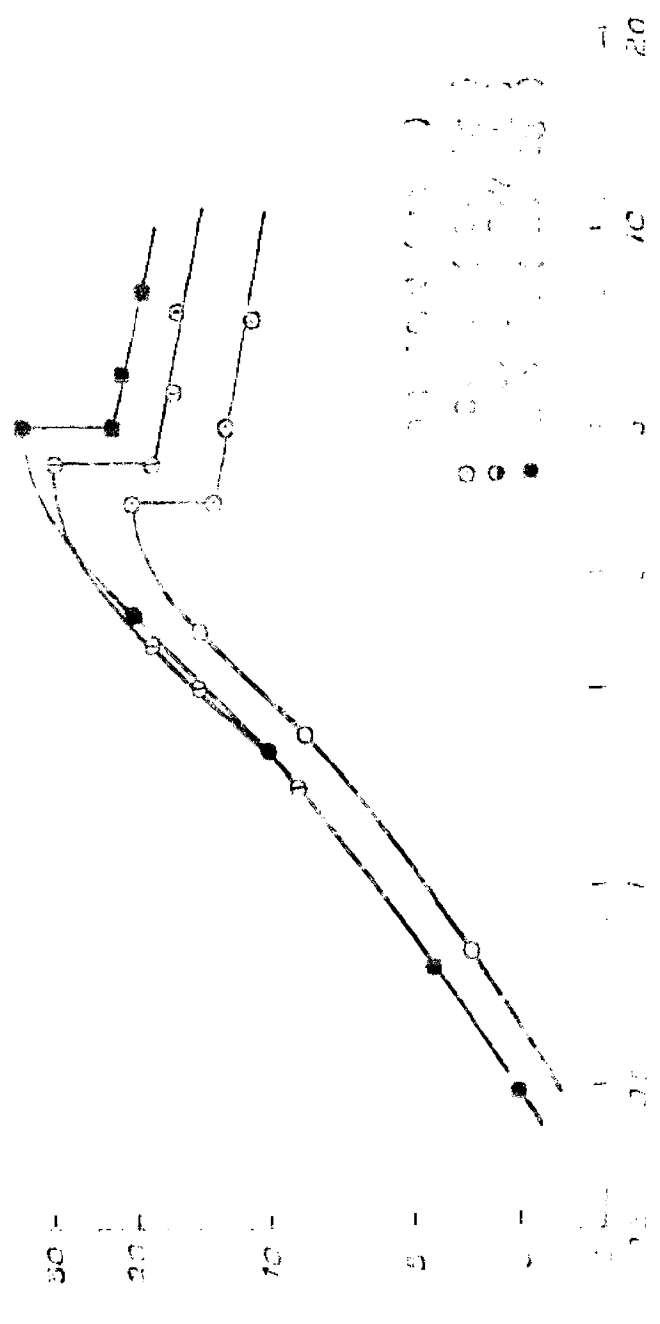
Sl. No.	Bed wt. kg.	Liq. flow rate, lit/min.	Manometer readings cm.		$\Delta P, \text{cm-CCl}_4$	Bed ht. cm.
1		0.6	46.2	44.0	2.2	10.6
2		1.5	47.9	42.2	5.7	10.6
3		2.0	49.6	40.5	9.1	10.6
4		2.6	51.9	38.1	13.8*	10.4
5	0.4	3.6	56.0	34.0	22.0*	10.3
6		3.6	52.0	38.0	14.0 ^x	11.0
7		4.0	51.7	38.3	13.4	11.5
8		5.8	51.0	39.0	12.0	11.0
<hr/>						
1		0.6	46.3	43.8	2.5	15.1
2		1.1	47.5	42.5	5.0	15.0
3		1.9	49.7	40.2	9.5	15.0
4	0.7	2.3	51.7	38.2	13.5*	15.0
5		4.0	60.0	30.0	30.0*	15.0
6		4.8	53.0	37.0	16.0 ^x	15.5
7		10.0	52.0	30.0	14.0	16.3
8						
<hr/>						
1		0.6	46.3	43.7	2.6	18.5
2		1.1	47.8	42.2	5.6	18.4
3		1.4	48.7	41.4	7.3	18.3
4		1.7	50.0	40.0	10.0	18.3
5	1.0	2.7	55.0	35.0	20.0*	18.2
6		6.0	63.0	27.0	36.0*	18.2
7		6.0	51.2	39.0	18.0 ^x	18.7
8		12.0	50.7	39.5	15.8	20.7

* Pressure peak (at limit of stability) for fixed bed.

x Pressure drop at onset of fluidization.

100 50 30 20 10 5 0

100 50 30 20 10 5 0



100 50 30 20 10 5 0

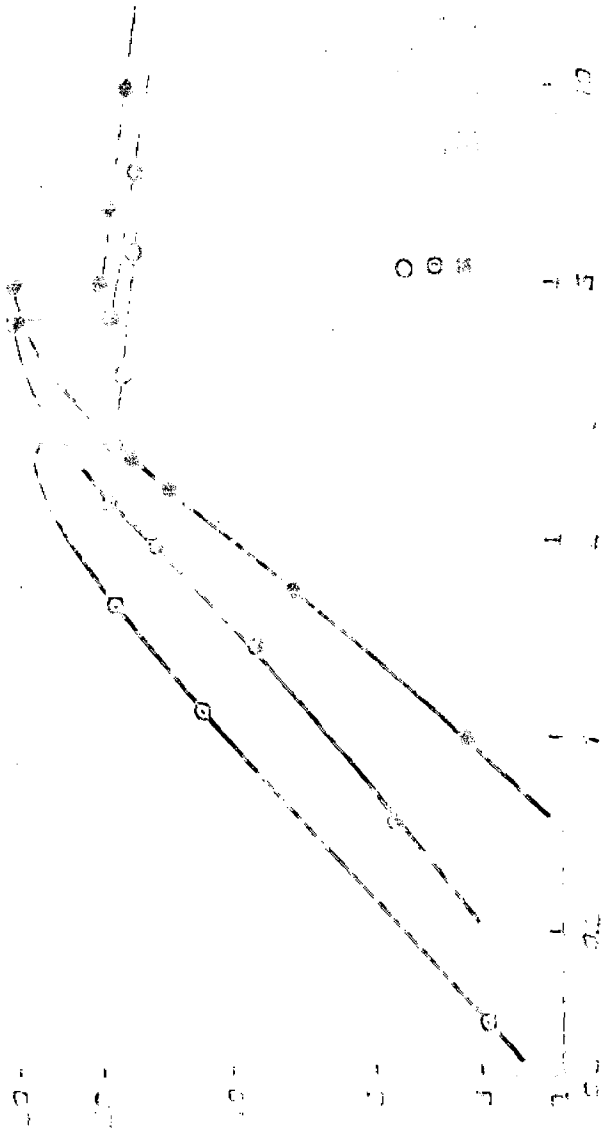
1950
 1951
 1952
 1953
 1954
 1955
 1956
 1957
 1958
 1959
 1960
 1961
 1962
 1963
 1964
 1965
 1966
 1967
 1968
 1969
 1970



0
 5
 10
 15
 20
 25
 30
 35
 40
 45
 50

0
 5
 10
 15
 20
 25
 30
 35
 40
 45
 50

100 -



100 90 80 70 60 50 40 30 20 10 0

1 2 3 4 5 6 7 8 9 10 11 12 13 14 15 16 17 18 19 20

Table No. 4.25

Cone angle, 30°

$$D_p = 0.1517 \text{ cm}$$

Material, Glass beads

$$P_0 = 2.5 \text{ gm/cc}$$

Mesh No. -10+12

$$\phi_s = 1$$

Sl. No.	Bed wt. kg.	Liq. flow rate lit/min.	Manometer readings cm.		$\Delta P, \text{cm-CCl}_4$	Bed ht. cm.
1	0.4	0.7	48.3	46.8	1.5	6.4
2		1.6	49.7	46.3	3.4	6.4
3		2.3	51.1	43.9	7.2	6.4
4		3.7	52.2	42.9	9.3 [*]	6.4
5		3.7	51.6	43.5	8.1 ^{**}	6.6
6		4.8	51.4	43.6	7.8	6.8
7		5.6	51.2	43.8	7.4	6.9
8		9.6	51.2	43.9	7.3	7.5
1	0.7	0.6	48.2	46.8	1.4	9.0
2		1.2	49.3	45.7	3.6	9.1
3		2.4	52.4	42.7	9.7	9.2
4		4.3	54.6	40.3	14.3 [*]	9.3
5		4.3	53.5	41.6	11.9 ^{**}	9.3
6		6.0	53.1	41.8	11.3	9.4
7		8.0	52.8	42.2	10.6	9.5
8		12.0	52.7	42.3	10.4	10.5
1	1.0	0.0	48.8	46.2	2.6	9.5
2		1.5	50.9	43.2	6.7	10.6
3		2.5	53.9	41.1	12.8	10.6
4		4.5	57.0	38.0	19.0 [*]	10.6
5		4.5	56.1	40.0	16.1 ^{**}	11.0
6		6.1	54.6	40.5	14.1	11.3
7		8.6	54.2	40.9	13.3	11.6
8		12.4	54.0	41.1	12.9	13.0
1	1.5	0.7	48.6	46.5	2.1	13.0
2		1.6	51.5	43.6	7.9	13.0
3		2.2	53.7	41.4	12.3	13.0
4		3.1	56.5	38.5	18.0 [*]	13.0
5		5.6	60.8	34.2	26.6 [*]	13.0
6		5.6	56.9	38.2	18.7 ^{**}	13.0
7		7.6	56.5	38.7	17.8	13.9
8		11.2	56.8	39.3	16.5	14.4
9		10.0	55.8	39.6	15.9	16.0

* Pressure peak (at limit of stability) for fixed bed.

** Pressure drop at onset of fluidization.

Table No. 4.26

Cone angle, 30°

$$D_p = 0.1617 \text{ cm}$$

Material, Quartz

$$\rho_s = 2.7 \text{ gm/cc}$$

Mesh No. -10+12

$$\phi_s =$$

Sl. No.	Bed wt. kg.	Liq. flow rate lit/min.	Manometer readings cm.		$\Delta P, \text{cm-CCl}_4$	Bed ht. cm.
1		0.7	48.1	47.4	0.7	7.2
2		2.0	49.3	46.1	3.2	7.0
3		2.8	50.3	45.2	5.1	7.0
4		3.2	50.3	44.7	5.6	7.0
5	0.4	5.4	53.1	42.4	10.7 ⁺	7.0
6		5.4	51.4	44.0	7.4 ^x	7.2
7		6.0	51.3	44.1	7.2	7.2
8		9.8	50.8	44.6	6.2	8.0
<hr/>						
1		0.5	48.0	47.5	0.5	9.8
2		1.4	49.1	46.4	2.7	9.7
3		2.7	51.1	44.5	6.6	9.7
4		3.9	53.1	42.4	10.7 ⁺	9.7
5	0.7	6.8	56.5	39.0	17.5 ⁺	9.7
6		6.8	53.1	42.5	10.6 ^x	10.1
7		8.5	52.8	42.8	10.0	10.2
8		13.0	52.0	43.6	8.4	11.1
<hr/>						
1		0.5	48.1	47.4	0.7	11.9
2		1.6	49.4	46.1	3.3	11.9
3		3.2	51.6	44.0	7.6	11.8
4		4.3	54.3	41.3	13.0	11.8
5	1.0	8.0	60.1	35.5	24.6 ⁺	11.8
6		8.0	54.1	41.6	12.5 ^x	12.3
7		11.2	53.4	42.1	11.3	12.7
8		15.2	52.8	42.7	10.1	13.5
<hr/>						
1.		0.4	48.1	47.3	0.8	14.9
2		1.9	49.9	45.7	4.2	14.8
3		4.2	54.2	41.4	12.8	14.6
4		4.4	56.2	39.4	16.8	14.5
5	1.5	9.2	65.6	30.0	35.6 ⁺	14.5
6		9.2	55.6	39.8	15.8 ^x	15.0
7		13.2	54.7	40.8	13.9	15.3
8		18.8	54.5	41.0	13.5	15.5

+ Pressure peak (at limit of stability) for fixed bed.

x Pressure drop at onset of fluidization.

Cone angle, 30°

 $D_p = 0.1517 \text{ cm}$

Material, Calcite

 $\rho_s = 2.7 \text{ gm/cc}$

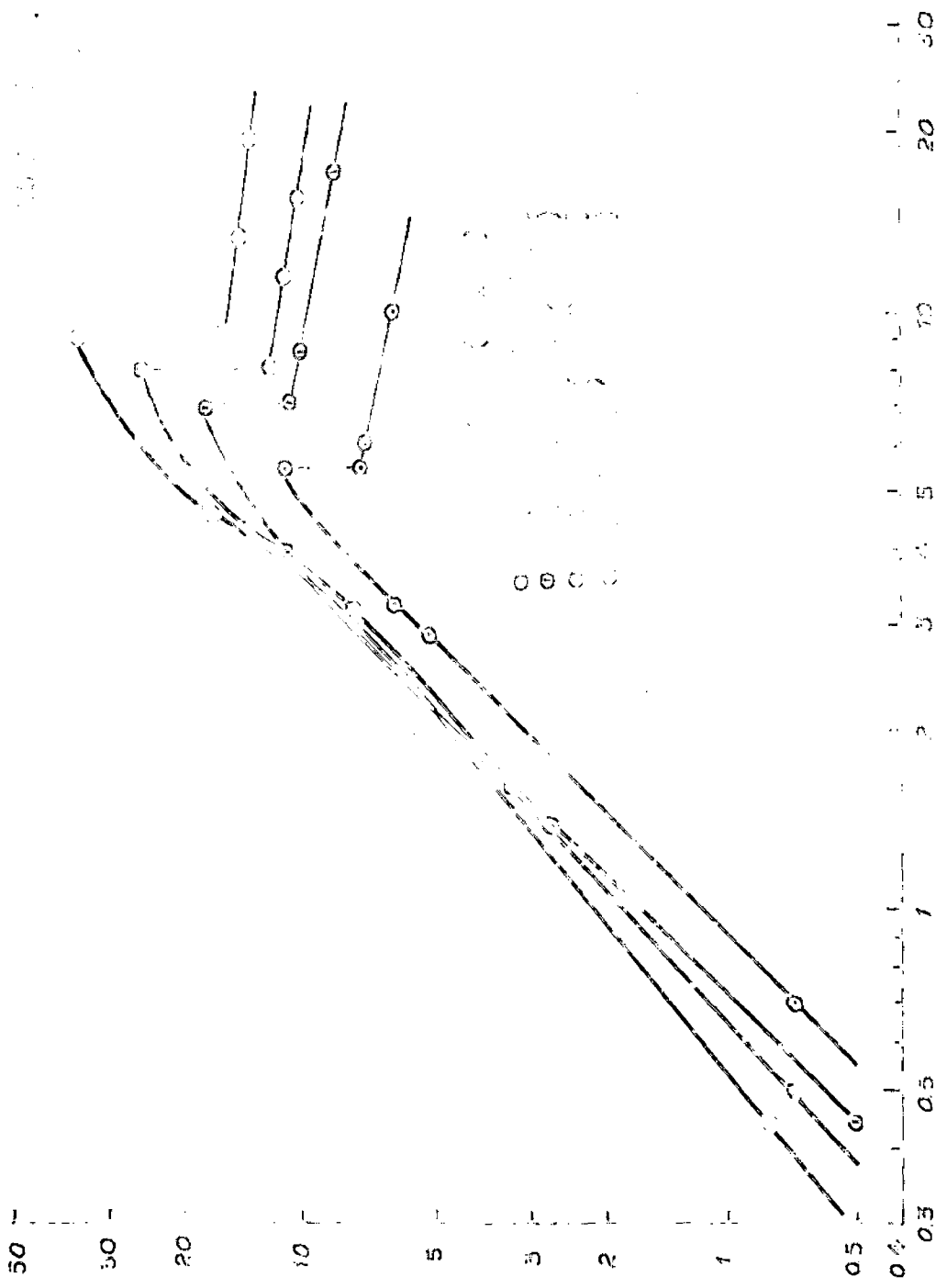
Mesh No., -Lo+12

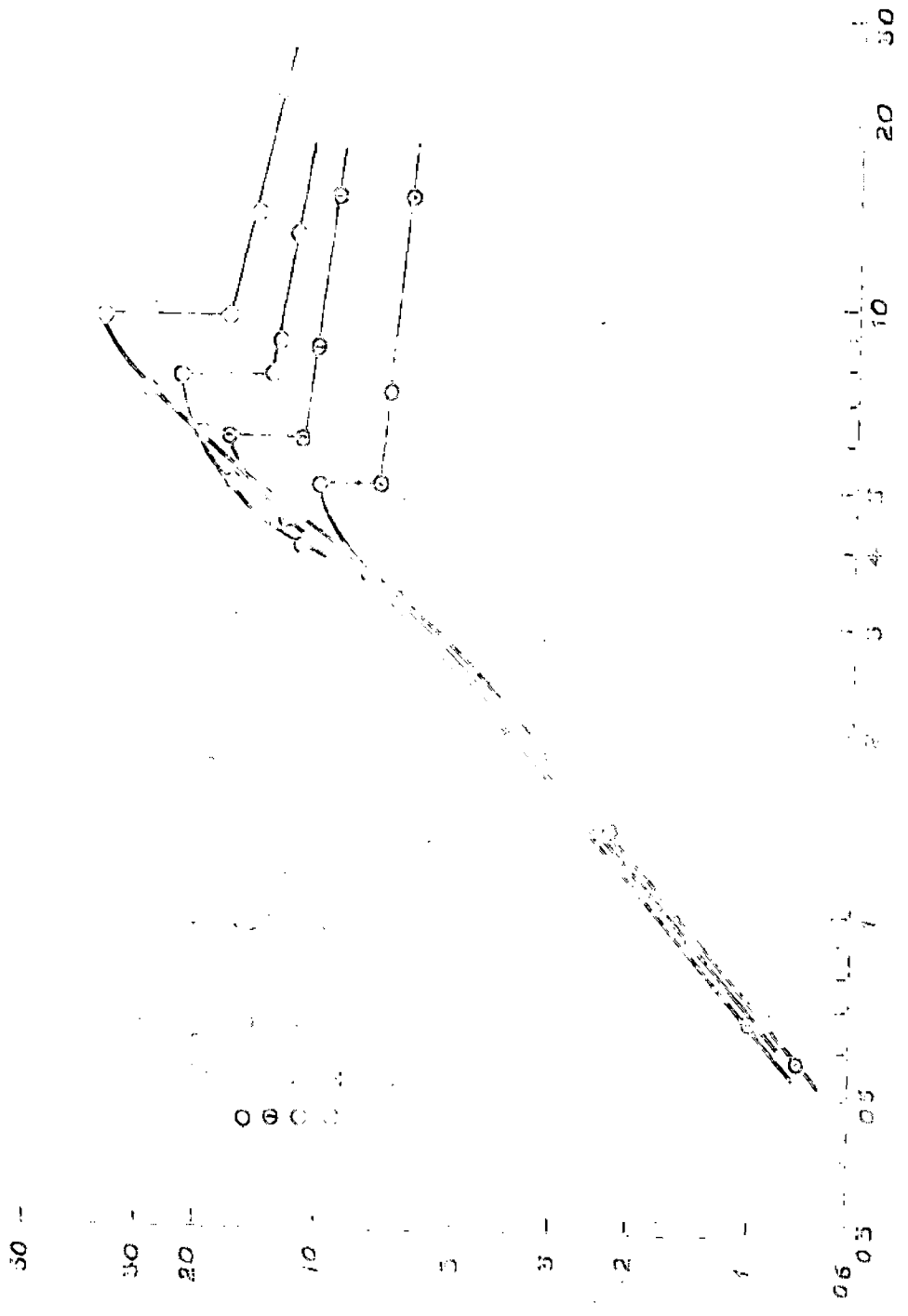
 $\phi_s =$

Sl. No.	Bed wt. kg.	Eq flow rate lit/min.	Manometer readings cm.		$\Delta P, \text{cm-CCl}_4$	Bed ht. cm.
1		0.6	48.2	47.4	0.8	7.0
2		1.4	48.9	46.7	2.2	7.0
3		3.3	51.2	44.4	6.8	6.9
4		3.6	51.8	43.8	8.0 ⁺	6.9
5		5.0	52.9	42.7	10.2 ⁺	6.8
6	0.4	5.0	51.6	44.0	7.6 ⁺	7.0
6		7.2	51.3	44.2	7.1	7.2
7		15.0	51.0	44.7	6.3	7.8
8						
1		0.6	43.3	47.3	1.0	9.5
2		1.9	49.7	46.0	3.7	9.5
3		3.4	51.6	44.0	7.6	9.5
4		4.4	54.1	41.6	12.5 ⁺	9.4
5	0.7	6.0	50.7	39.0	11.7 ⁺	9.4
6		6.0	53.6	42.2	11.4 ^x	9.7
7		8.4	53.0	42.6	10.4	9.0
8		15.0	52.6	43.1	9.5	11.2
9						
1		0.9	48.5	47.1	1.4	11.6
2		2.2	47.8	45.8	4.0	11.4
3		3.6	51.8	43.9	7.9	11.4
4		4.0	53.4	42.3	11.1	11.3
5	1.0	5.1	56.4	39.2	17.2 ⁺	11.2
6		7.6	59.1	36.6	22.6 ⁺	11.1
7		7.6	54.8	40.9	13.9 ^x	11.7
8		8.6	54.3	41.3	13.0	11.8
9		12.8	53.7	41.9	11.8	12.4
10						
1		0.7	40.3	47.4	0.9	14.5
2		2.0	40.5	40.2	3.3	14.4
3		3.4	51.7	43.9	7.8	14.3
4		4.7	46.0	41.6	12.4	14.2
5	1.5	6.1	57.9	37.7	20.2	14.2
6		7.1	61.2	34.4	26.8 ⁺	14.1
7		9.4	64.6	31.0	33.6 ⁺	14.1
8		9.4	56.5	39.0	17.5 ^x	14.6
9		14.0	55.2	40.3	14.9	14.9
10		22.8	54.4	41.2	13.2	16.0

† Pressure peak (at limit of stability) for fixed bed.

x Pressure drop at onset of fluidization.





0.5

Table No. 4-23

Cone angle, 45° $D_p = 0.1517 \text{ cm}$
 Material, Glass beads $\rho_s = 2.5 \text{ gm/cc}$
 Mesh No., -10+12 $\phi_s = 1$

Sl. No.	Bcd wt. kg.	Liq. flow rate lit/min.	Manometer readings cm.		$\Delta P, \text{cm-CCl}_4$	Bcd ht. cm.
1	0.5	1.1	48.5	47.2	1.3	8.1
2		1.4	48.8	47.1	1.7	8.1
3		2.4	49.8	46.1	3.7	8.1
4		3.9	51.1	44.8	6.3	8.1
5		4.7	51.9	44.0	7.9 ⁺	8.1
6		4.7	51.1	44.8	6.7 ⁺	8.1
7		6.9	50.7	45.2	5.5	8.1
8		11.2	50.6	45.3	5.3	8.1
1	1.0	0.7	48.3	47.5	0.8	9.7
2		1.8	49.1	46.7	2.4	9.7
3		3.4	50.5	45.4	5.1	9.7
4		4.0	51.6	44.2	7.4 ⁺	9.7
5		6.5	55.8	40.0	15.8 ⁺	9.7
6		6.5	52.3	43.1	9.2 ⁺	9.7
7		8.4	52.3	43.5	8.8	9.7
8		11.4	52.1	43.7	8.4	9.7
1	1.5	0.9	48.6	47.5	1.1	10.6
2		1.8	49.4	46.7	2.7	10.6
3		3.5	51.2	44.8	6.4	10.6
4		4.6	53.5	42.6	10.9	10.6
5		5.6	55.5	40.6	14.9 ⁺	10.6
6		8.0	56.6	39.5	22.0 ⁺	10.6
7		8.0	54.1	41.9	12.0 ⁺	10.6
8		10.3	53.4	42.6	10.8	10.6
9		20.8	53.1	42.9	10.2	10.6

† Pressure peak (at limit of stability) for fixed bcd.

‡ Pressure drop at onset of fluidization.

Cono angle, 45° $D_p = 0.1517$ cm
 Material, quartz $\rho_s = 2.7$ gm/cc
 Mesh No., -10+12 $\phi_s =$

Sl. No.	Bed wt. kg.	Liq. flow rate, lit/min.	Manometer readings cm.		$\Delta P, \text{cm-CCl}_4$	Bed ht. cm.
1		1.4	48.4	47.7	0.7	6.9
2		3.0	49.0	47.2	1.8	6.9
3		4.4	50.0	46.2	3.8	6.9
4	0.5	6.5	52.2	43.8	8.4 [*]	6.9
5		6.5	50.5	45.7	4.8 ^{**}	6.9
6		9.0	50.3	45.8	4.5	6.9
7		14.8	50.0	46.0	4.0	6.9
1		1.0	48.4	47.7	0.7	9.7
2		3.1	49.6	46.4	3.2	9.7
3		5.9	52.5	43.5	9.0 [*]	9.7
4	1.0	9.0	56.2	39.8	16.4 [*]	9.7
5		9.0	51.7	44.3	7.4 ^{**}	9.7
6		15.0	51.3	44.7	6.6	9.7
7		26.0	51.0	44.9	6.1	9.7
1		0.9	48.2	47.7	0.5	12.9
2		4.0	49.8	46.0	3.8	12.9
3		7.0	53.4	42.5	10.9 [*]	12.9
4	1.5	12.4	59.1	36.8	22.3 [*]	12.9
5		12.4	52.9	42.9	10.0 ^{**}	12.9
6		14.4	52.3	43.5	8.8	12.9
7		24.0	51.9	43.9	8.0	12.9

* Pressure peak (at limit of stability) for fixed bed.

** Pressure drop at onset of fluidization.

Table No. 4.30

67

Cone angle, 45°

$$D_p = 0.1517 \text{ cm}$$

Material, Calcite

$$\rho_s = 2.7 \text{ gm/cc}$$

Mesh No., -10+12

$$\phi_s =$$

Sl. No.	Bed wt. kg.	Liq. flow rate, lit/min.	Manometer readings cm.		$\Delta P, \text{cm-CCl}_4$	Bed ht. cm.
1		1.8	48.1	47.3	0.8	6.5
2		3.5	48.7	46.7	2.0	6.5
3		5.3	49.6	45.6	4.2	6.5
4		6.5	51.1	44.3	6.8 ⁺	6.5
5	0.5	9.6	52.4	43.0	9.4 ⁺	6.5
6		9.6	50.3	45.2	5.1 ^x	6.5
7		15.0	49.9	45.0	4.3	6.5
8		20.0	49.6	45.9	3.7	6.5
1		2.0	48.3	47.2	1.1	9.8
2		4.0	49.2	46.2	3.0	9.8
3	1.0	7.8	52.0	43.6	8.5 ⁺	9.8
4		12.0	55.8	41.7	14.1 ⁺	9.8
5		12.0	51.5	43.8	7.7 ^x	9.8
6		16.8	50.9	44.4	6.5	9.8
7		23.0	50.5	44.9	5.6	9.8
1		1.6	47.9	46.9	1.0	11.8
2		3.8	49.2	45.6	3.6	11.8
3		6.6	51.7	43.1	8.6	11.8
4		8.4	53.5	41.2	12.3 ⁺	11.8
5	1.5	14.0	58.4	36.3	22.1 ⁺	11.8
6		14.0	52.1	42.6	9.5 ^x	11.8
7		19.2	51.7	43.1	8.6	11.8
8		25.0	51.4	43.4	8.0	11.8

⁺ Pressure peak (at limit of stability) for fixed bed.

^x Pressure drop at onset of fluidization.

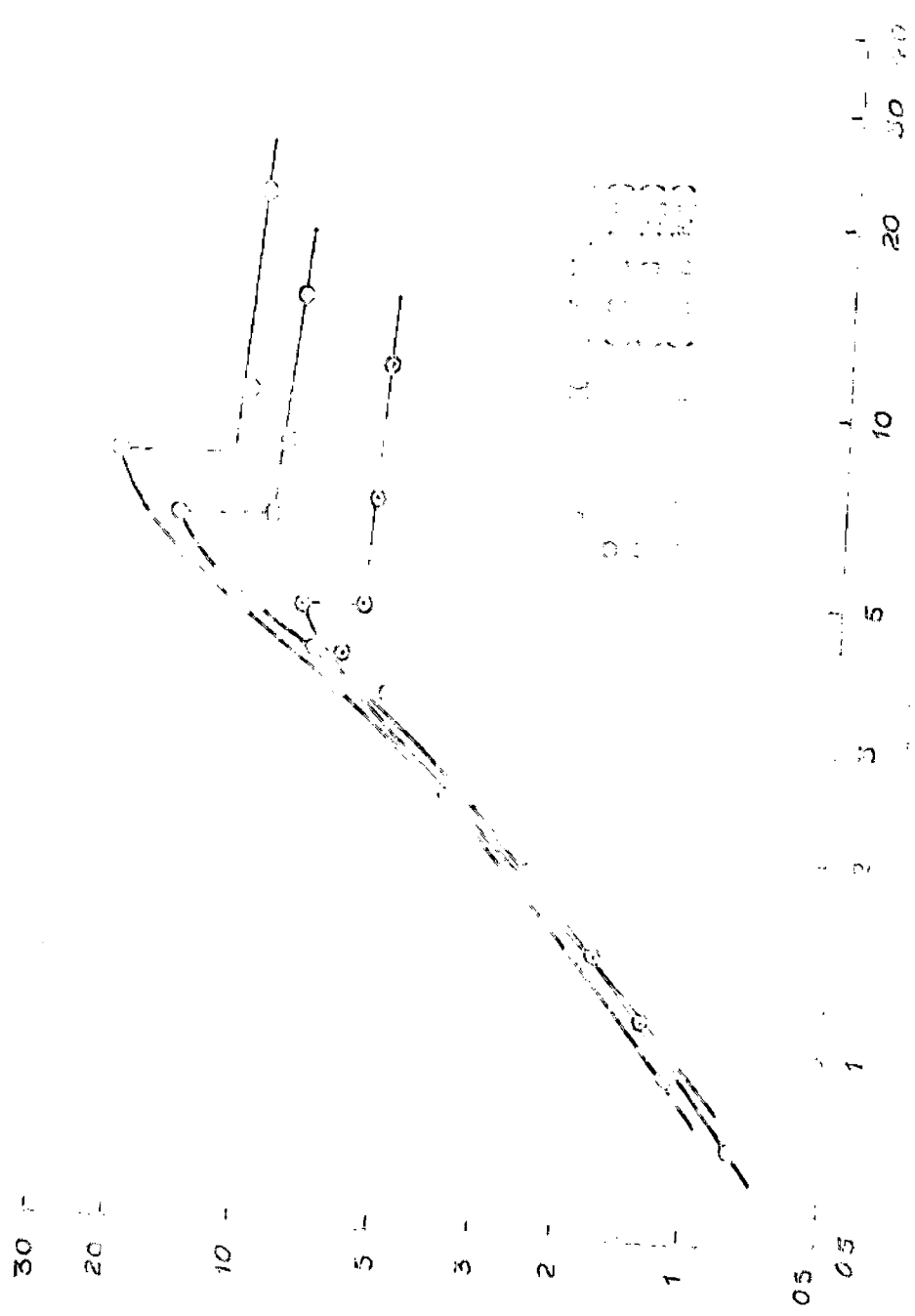


Figure 1. Comparison of the results of the model with the experimental data.

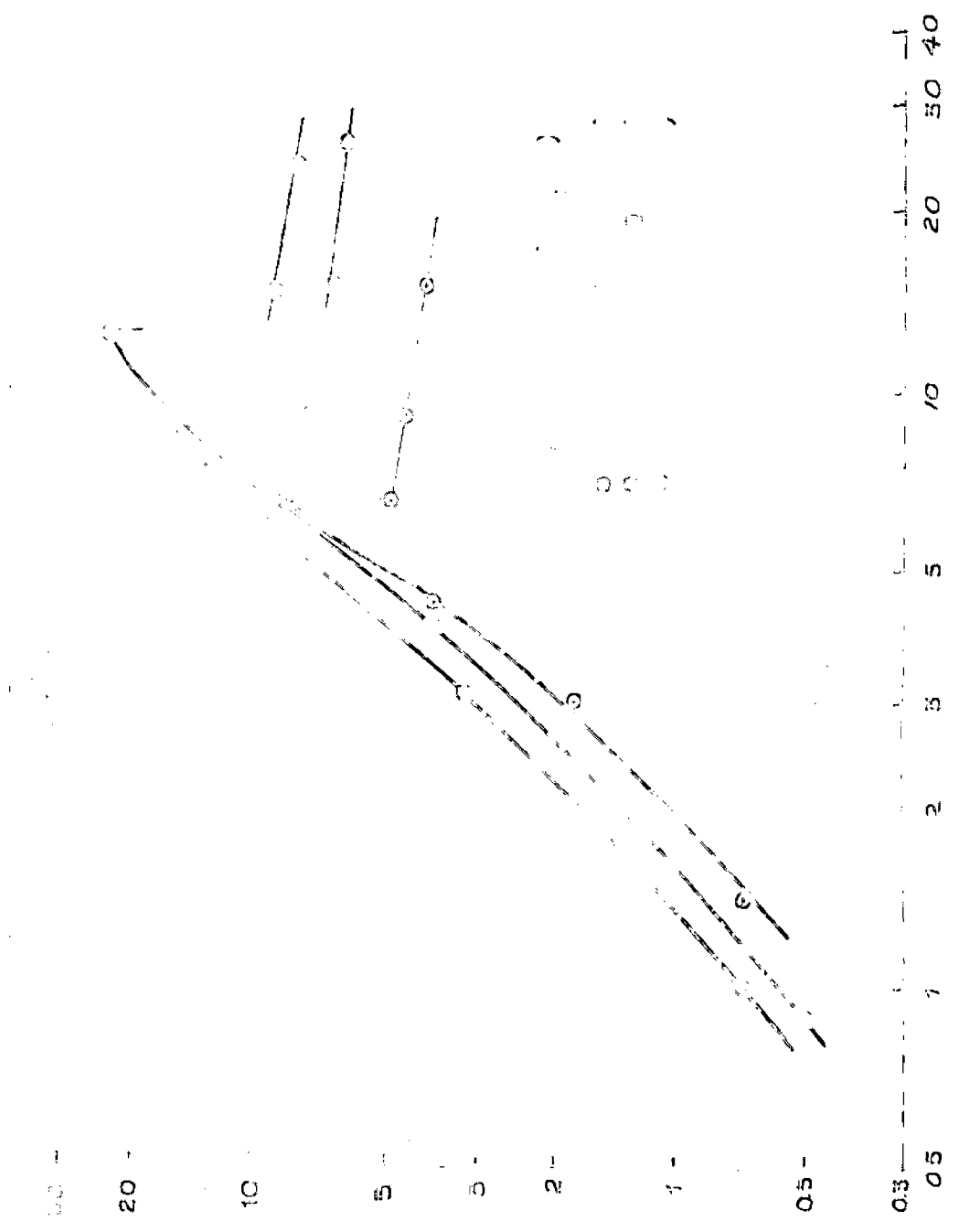


Figure 1

100 - 20 - 10 - 5 - 5 - 2 - 1 - 0.5 - 0.3 - 0.5 1 2 5 10 20 50 40

10

20

30

40

50

60

70

80

90

100



10
20
30
40

50

60

70

80

90

100

Table No. 4.11

Cone angle, 90° $D_p = 0.1517 \text{ cm}$

Material, Glass beads

 $\rho_s = 2.5 \text{ gm/cc}$

Mesh No., 10+12

 $\phi_s = 1$

Sl. No.	Bed wt. gk.	Liq. flow rate, lit/min.	Manometer readings cm.		$\Delta P, \text{cm-CCl}_4$	Bed ht. cm.
1	0.5	1.2	48.2	47.4	0.8	5.0
2		2.0	48.9	46.7	2.2 ⁺	5.0
3		3.4	50.2	46.4	4.1 ⁺	5.0
4		5.4	49.2	46.4	2.8 ⁺	5.0
5		4.8	49.2	46.5	2.7	5.0
6		10.0	49.2	46.5	2.7	5.0
1	1.0	1.2	48.3	47.4	0.9	5.9
2		2.8	49.5	46.3	3.2 ⁺	5.9
3		6.0	51.5	44.3	7.2 ⁺	5.9
4		6.0	50.1	45.6	4.5 ⁺	5.9
5		9.6	50.0	45.7	4.3	5.9
6		16.0	49.9	45.7	4.2	5.9
7		23.0	49.9	45.8	4.1	5.9
1	1.5	1.6	48.5	47.2	1.3	6.7
2		3.4	49.6	46.1	3.5	6.7
3		4.6	50.4	45.3	5.1 ⁺	6.7
4		8.0	52.2	43.5	8.7 ⁺	6.7
5		8.0	50.5	46.2	5.3 ⁺	6.7
6		12.8	50.3	45.4	4.9	6.7
7		12.0	50.3	45.4	4.9	6.7

† Pressure peak (at limit of stability) for fixed bed.

π Pressure drop at onset of fluidization.

Table No. 4.32

Cone angle, 90°

$$D_p = 0.1517 \text{ cm}$$

Material, Quartz

$$\rho_s = 2.7 \text{ gm/cc}$$

Mesh No., -10+12

$$\phi_s =$$

Sl. No.	Bcd wt. kg.	Liq. flow rate lit./min.	Manometer readings cms.		ΔP , gm- CCl_4	Bcd ht. cm.
1	0.5	1.4	47.6	47.2	0.4	5.5
2		2.3	47.9	46.8	1.1	5.5
3		4.0	48.9	46.0	2.9 _y	5.5
4		6.6	50.0	44.7	5.3 _y	5.5
5		9.0	48.5	46.3	2.2 _x	5.5
6		10.0	48.3	46.5	1.8	5.5
7		17.0	48.2	46.6	1.6	5.5
1	1.0	1.6	47.8	47.1	0.7	6.6
2		2.8	48.4	46.4	2.0	6.6
3		6.8	50.5	46.4	5.1 _y	6.6
4		10.0	51.0	45.0	6.0 _x	6.6
5		10.0	49.0	45.8	3.2 _x	6.6
6		14.0	48.8	46.0	2.8	6.6
7		24.0	48.7	46.1	2.6	6.6
1	1.5	1.4	47.7	47.1	0.6	7.4
2		2.3	48.2	46.6	1.6	7.4
3		5.8	50.0	44.8	5.2 _y	7.4
4		13.6	51.8	43.0	8.8 _y	7.4
5		13.6	49.4	45.6	3.8 _x	7.4
6		18.4	49.1	45.8	3.3	7.4
7		28.0	49.0	45.9	3.1	7.4

* Pressure peak (at limit of stability) for fixed bed.

x Pressure drop at onset of fluidization.

Table No. 4.33

70

Cone angle, 90° $D_p = 0.1517 \text{ cm}$

Material, Calcite

 $\rho_s = 2.7 \text{ gm/cc}$

Mesh No., -10+12

 $\phi_s =$

Sl. No.	Bed wt. kg.	Liq. flow rate, lit/min.	Manometer readings cms.		$\Delta P, \text{cm-CCl}_4$	Bed ht. cm.
1		2.2	48.3	47.3	1.0	5.5
2		3.1	48.8	46.9	1.9	5.5
3		6.4	49.9	45.8	4.1 [*]	5.5
4	0.5	6.4	49.0	46.5	2.5 ^x	5.5
5		11.3	48.9	46.7	2.2	5.5
6		24.0	48.8	46.8	2.0	5.5
1		1.6	48.2	47.4	0.8	6.9
2		2.5	48.8	46.8	2.0	6.9
3		5.2	50.5	45.0	5.5 [*]	6.9
4	1.0	10.4	51.5	44.0	7.5 ^x	6.9
5		10.4	50.0	45.7	4.3 ^x	6.9
6		14.8	49.5	46.1	3.4	6.9
7		26.0	49.2	46.4	2.8	6.9
1		2.0	48.3	47.3	1.0	7.8
2		4.6	49.8	45.7	4.1	7.8
3		7.7	51.4	44.3	7.1 [*]	7.8
4	1.5	16.0	52.7	43.0	9.7 ^x	7.8
5		16.0	50.0	45.6	4.4 ^x	7.8
6		20.0	49.8	45.8	4.0	7.8
7		30.0	49.6	46.0	3.6	7.8

* Pressure point (at limit of stability) for fixed bed.

x Pressure drop at onset of fluidization.



Figure 1. Comparison of the two data series over 60 days. The solid line with open circles represents Series 1, and the dashed line with open circles represents Series 2. Both series show an initial rapid increase followed by fluctuations between 5 and 10.

Table No. 4.34

Cone angle, 120° $D_p = 0.1617 \text{ cm}$

Material, Glass beads

 $\rho_s = 2.5 \text{ gm/cc}$

Koch No. 10+12

 $\phi_s = 1$

Sl. No.	Bed wt. kg.	Liq. flow rate, lit/min.	Manometer readings cms.		$\Delta P, \text{cm-CCl}_4$	Bed ht. cm.
1		1.0	30.3	29.9	0.4	3.2
2		2.0	30.5	29.8	0.7	3.3
3		3.4	31.0	29.3	1.7 [*]	3.2
4	0.5	3.4	30.9	29.6	1.4 ^{II}	3.2
5		6.0	30.8	29.6	1.2	3.2
6		16.0	30.7	29.7	1.0	3.2
1		1.3	30.5	29.8	0.7	4.0
2		2.4	31.2	29.3	1.9	4.0
3		3.8	31.6	28.9	2.7 [*]	4.0
4	1.0	3.8	31.3	29.2	2.1 ^{II}	4.0
5		6.0	31.2	29.2	2.0	4.0
6		10.8	31.2	29.3	1.9	4.0
1		1.6	30.7	29.9	0.8	4.7
2		2.7	31.6	28.9	2.7 [*]	4.7
3		4.2	32.7	27.8	4.9	4.7
4	1.5	4.2	31.8	28.8	3.0 ^{II}	4.7
5		7.0	31.6	28.9	2.7	4.7
6		24.0	31.4	29.1	2.3	4.7

* Pressure peak (at limit of stability) for fixed bed.

II Pressure drop at onset of fluidization.

Table No. 4.35

Cone angle, 120°

$D_p = 0.1517 \text{ cm}$

Material, Quartz

$\rho_s = 2.7 \text{ gm/cc}$

Mesh No. $10+12$

$\phi_s =$

Sl. No.	Bed wt. gk.	Liq. flow rate, lit/min.	Manometer readings cmg.	$\Delta P, \text{cm-CCl}_4$	Bed ht. cm.	
1	0.5	1.7	30.5	29.9	0.6	3.2
2		2.5	30.8	29.6	1.2	3.2
3		3.9	31.3	29.1	2.2 [*]	3.2
4		3.0	30.9	29.7	1.2 [*]	3.2
5		7.0	30.8	29.8	1.0	3.2
6		16.8	30.7	29.8	0.9	3.2
1	1.0	1.9	30.6	29.9	0.7	4.3
2		3.3	31.7	29.9	2.0 [*]	4.3
3		5.8	32.2	28.4	3.0 [*]	4.3
4		5.8	31.2	29.3	1.9 [*]	4.3
5		17.6	31.1	29.5	1.6	4.3
1	1.5	2.0	30.7	29.9	0.8	5.0
2		3.0	31.3	29.3	2.0	5.0
3		4.4	31.9	28.7	3.2 [*]	5.0
4		6.3	32.6	28.0	4.6 [*]	5.0
5		6.3	31.3	29.3	2.0 [*]	5.0
6		10.0	31.2	29.3	1.9	5.0

* Pressure peak (at limit of stability) for fixed bed.

x Pressure drop at onset of fluidization.

Table No. 4.36

Cone angle, 120°

$$D_p = 0.1517 \text{ cm}$$

Material, Celeite

$$\rho_s = 2.7 \text{ gm/cc}$$

Mash No., -10+12

$$\phi_s =$$

Sl. No.	Bed wt. kg.	Liq. flow rate, lit/min.	Manometer readings cms.		$\Delta P, \text{um-CCl}_4$	Bed ht. cm.
1		1.4	30.5	30.0	0.5	3.4
2		2.0	30.7	29.7	1.0	3.4
3		4.0	31.5	29.0	2.5 [†]	3.4
4	0.5	4.0	31.0	29.6	1.4 ^π	3.4
5		7.0	30.95	29.6	1.35	3.4
6		16.0	30.9	29.6	1.3	3.4
1		1.6	30.5	29.9	0.6	4.2
2		3.6	31.4	29.1	2.3	4.2
3	1.0	0.8	32.6	27.9	4.7 [†]	4.2
4		6.2	31.3	29.1	2.2 ^π	4.2
5		16.0	31.1	29.3	1.8	4.2
1		1.8	30.5	29.8	0.7	5.0
2		4.0	31.6	28.8	2.8	5.0
3	1.5	7.2	33.0	27.4	5.6 [†]	5.0
4		7.8	31.8	28.7	3.1 ^π	5.0
5		19.0	31.4	29.0	2.4	5.0

† Pressure peak (at limit of stability) for fixed bed.

π Pressure drop at onset of fluidization.



Figure 1: A graph showing the relationship between the x-axis (ranging from 0.0 to 1.0) and the y-axis (ranging from 0.5 to 10.0). The curves represent different data series, labeled 0.5, 0.5, 1, 2, and 3. The curves generally decrease as the x-axis value increases, with some showing a sharp drop at x=0.5.

CHAPTER 5

CONCLUSIONS

Experimental studies were carried out in tapered vessels with apex angle ranging from 10° to 120°, to investigate the optimum cone angle for solid-liquid contact. Based on experimental studies using glass beads, calcite and quartz of different particle sizes it has been observed that a cone angle greater than 45° adversely affects the solid-liquid contact. In vessels having a cone angle more than 45° the particle movement is limited to a central core with particles remaining stationary in a thick layer adjacent to the vessel wall.

It has been observed that increase in bed height increases the pressure peak value. For the same particle size pressure peak is more for crushed materials than for spherical particles. Pressure peak is more in case of material having size distribution than for a material of uniform size.

Pressure peak is a characteristic of solid-fluid contact in tapered vessels, which is not so prominent in case of cylindrical vessels. The pressure peak in conical vessels is comparable in value to the net bed weight pressure drop. Pressure peak has been correlated in terms of $\tan \alpha/2$, D/D_0 and Re_{pmf} based on the entrance. The correlation given below is valid for conical vessels ranging from 10° to 45° for spherical as well as crushed materials in size range -10+12 to -16+18 mesh nos.

$$(\Delta P/\Delta P) = 1.02 \times 10^{-3} (D/D_0)^{1.63} (\tan \alpha/2)^{-1.25} (D_p G_{mf}/\mu)^{0.712}$$

The percentage deviation has been found to be $\pm 35\%$.

REFERENCES

1. Levoy, R.P., et al, "Fluid bed conversion of UO_2 to UF_4 ", Chem. Eng. Progr., 56(3), 43-48 (1960).
2. Brots, W., Chem - Ing - Tech., 24, 60 (1962).
3. Roden, G.H., Chem and Ind. (Rev.), p. 46 (1955).
4. Sutherland, K.S., "Solids mixing studies in the gas fluidized beds Part I A preliminary comparison of tapered and non-tapered beds", Trans. Inst. Chem. Engrs., 39, 189-194 (1961).
5. Sutherland, K.S., and Rowe, P.H., Trans. Inst. Chem. Engrs., 42, 65 (1964).
6. Ridgway, K., "The tapered fluidized bed a new processing tool", Chem and Proc-Eng., June 1965, p. 317.
7. Ergun, S., Chem. Eng-Prog., 48(2), 89-94 (1952).
8. Gal'perin, et al., Khim. i Tekhnol. Topliva i Gazov, 5 (8), 51-57 (1960).
9. Tailby, S.R., and Coquerel, M.A.T., Trans. Inst. Chem. Engrs., 39, 195 (1961).
10. Gilliland, R.R., and Mason, E.A., Ind. and Eng-Chem., 41, 1101 (1949); 44, 218 (1952).
11. MacMullin, R., and Weber, M., Trans. A.I.Ch.E. J., 31, 409 (1936).
12. Romero, J.B., and Johanson, L.H., Chem. Eng. Progr. Symp. Ser., 58 (38), (Oct. 1962).
13. Littman, H., "Solids mixing in straight and tapered fluidized beds", A.I.Ch.E. J., 10(6), 924-929 (1964).
14. Farkas, E.J., and Koloini, T., "Fixed bed pressure drop and liquid fluidization in tapered or conical vessels", Can. J. Chem. Eng., 51, 499-502 (1973).
15. Gorshotin, A.D., and Mukhlenov, I.P., Zh. Fiz. Khim., 37 (9), 1887-1893 (1964).
16. Baskakov, A.P., Gal'perin, L.G., Inzh. Fiz. Zh., 9 (2), 217-222 (1965).
17. Kolar, V., Coll. Czech. Chem. Comm., 28, 1220-1231 (1963).
18. Richardson, J.F., and Zaki, W.H., "Sedimentation and fluidization", Trans. Inst. Chem. Engrs., 32, 35-63 (1954).

19. McCune, L.K., and Wilhelm, R.H., Ind. and Eng. Chem., 41, 1124 (1949).

20. Lewis, E.W., and Bowerman, E.U., Chem. Eng. Progr., 48, C03 (1952).

21. Onoe, T., and Furukawa, J.J. Chem., Soc. Japan, Ind. Chem. Section, 86 (12), 824 (1953).

22. Coulson, J.M. and Richardson, J.F., "Chem. Engg.", Pergamon Press, London, 2, 286 (1955).

23. McCabe, W.L., and Smith, J.C., "Unit Operations of chemical Engineering", McGraw Hill Book Co., Inc., Second Ed. (1967).

24. Epton, G.G., and Associates, "Unit Operations", Charles E. Tuttle Co., Tokyo, Modern Asia Ed. (1967).

25. Zabrodsky, S.S., "Hydrodynamics and Heat Transfer in fluidized beds", M.I.T. Press, (1966).

26. Kunii, D., and Levenspiel, O., John Wiley and Sons, Inc., (1969).

NOMENCLATURE

- $A = (\mu/g_c D_p^3) (1 - \epsilon)^2 / \epsilon^3$
- A_{avg} = Average cross-sectional area of the bed.
- a_0 = distance normal to the longitudinal axes of the column between tapered sides.
- $B = (\rho_f/g_c D_p) (1 - \epsilon) / \epsilon^3$
- C = constant in equation (8).
- C_1, C_2 = coefficients in Ergun type equation (4 and 9).
- C_D = Drag coefficient in equation (19).
- D, D_0 = Bed diameters at the top and bottom of the bed respectively.
- D_p = Particle diameter.
- F = Drag force on the particles in equation (19).
- g = Acceleration due to gravity.
- g_c = Gravitational constant.
- k = coefficient in equation (7).
- L, l = Bed heights from bottom of the bed to the top and upto some intermediate point respectively.
- L_{mf} = Bed height at the minimum fluidization.
- M = Mass of the solid particles charged to the bed.
- ΔP = Pressure drop across the bed, frictional.
- P_b, P_t = Pressures at the base and top of the bed respectively.
- R, R_0 = Radial distance from the apex of the cone to the top of the bed and upto the distributor respectively.
- r_b, r_t, r = Bed radius at the base, top and at an intermediate point of the bed respectively.

- U_0 = Superficial fluid velocity at the distributor.
- U_t = Terminal velocity of the particles.
- W_{net} = Net weight or buoyant weight of material in the bed.
- x = Exponent in equation (14).
- ϵ = Bed porosity.
- ρ_s, ρ_f, ρ_b = Densities of the solid particles, fluid and of the bed (bulk) respectively.
- α = apex angle of the cone.
- μ = fluid viscosity.
- Δw = Pressure peak in the tapered vessels.
- ϕ_s = particle shape factor.

APPENDIX

PROGRAMMES FOR LEAST SQUARE CURVE FITTING

```

C C PROGRAMME NO. 1
C C ME THESIS ISHWAR CHANDRA CHEMICAL UOR
  DIMENSION Y(70),X1(70),X2(70),X3(70)
  READ5,N
  5 FORMAT(I5)
  READ10,(Y(I),X1(I),X2(I),X3(I),I=1,N)
  10 FORMAT(4F15.5)
  DO15I=1,N
  Y(I)=LOGF(Y(I))
  X1(I)=LOGF(X1(I))
  X2(I)=LOGF(X2(I))
  X3(I)=LOGF(X3(I))
  15 CONTINUE
  SMY=0.0 $ SMX1=0.0 $ SMX2=0.0 $ SMX3=0.0
  DO20I=1,N
  SMY=SMY+Y(I)
  SMX1=SMX1+X1(I)
  SMX2=SMX2+X2(I)
  SMX3=SMX3+X3(I)
  20 CONTINUE
  AN=N
  YM=SMY/AN
  XM1=SMX1/AN
  XM2=SMX2/AN
  XM3=SMX3/AN
  PUNCH30,YM, XM1, XM2, XM3
  30 FORMAT(5X,3HYM=,F10.4,2X,4HXM1=,F10.4,2X,4HXM2=,F10.4,2X,4HXM3=,
  1F10.4)
  S1=0.0 $ S2=0.0 $ S3=0.0 $ S4=0.0
  S6=0.0 $ S7=0.0 $ S8=0.0 $ S11=0.0 $ S12=0.0
  DO40I=1,N
  ZY=Y(I)-YM
  Z1=X1(I)-XM1
  Z2=X2(I)-XM2
  Z3=X3(I)-XM3
  S1=S1+Z1*Z1
  S2=S2+Z1*Z2
  S3=S3+Z1*Z3
  S4=S4+Z1*ZY
  S6=S6+Z2*Z2
  S7=S7+Z2*Z3
  S8=S8+Z2*ZY
  S11=S11+Z3*Z3
  S12=S12+Z3*ZY
  40 CONTINUE
  S5=S2
  S9=S3
  S10=S7
  PUNCH50,S1,S2,S3,S4
  50 FORMAT(/5X,3HS1=,F10.4,2X,3HS2=,F10.4,2X,3HS3=,F10.4,2X,
  13HS4=,F10.4//)

```



```

PUNCH60,S5,S6,S7,S8
60 FORMAT(/5X,3HS5=,F10.4,2X,3HS6=,F10.4,2X,3HS7=,F10.4,2X,
13HS8=,F10.4//)
PUNCH70,S9,S10,S11,S12
70 FORMAT(/5X,3HS9=,F10.4,2X,4HS10=,F10.4,2X,4HS11=,F10.4,2X,
14HS12=,F10.4//)
STOP
END

```

67

0.26	1.68	.125	56.0
1.17	1.98	.085	120.0
0.88	1.9	.085	100.0
0.8	1.56	.085	90.0
0.61	2.0	.125	70.0
0.66	2.21	.125	85.0
0.28	1.32	.16	56.0
0.47	2.16	.16	68.0
0.68	2.4	.16	80.0
0.71	1.56	.085	33.0
0.79	1.3	.085	38.0
1.19	1.98	.085	47.0
0.15	1.38	.125	20.0
0.52	2.0	.125	26.0
0.54	2.21	.125	32.0
0.24	1.8	.16	22.0
0.28	2.12	.16	27.0
0.32	2.35	.16	33.0
0.16	1.9	.28	74.0
0.22	2.26	.28	86.0
0.27	2.37	.28	91.0
0.64	2.32	.28	113.0
0.84	3.3	.435	160.0
0.72	3.11	.435	130.0
0.39	2.76	.435	95.0
.57	1.34	.16	72.0
.88	2.2	.16	96.0
1.0	2.38	.16	120.0
.35	1.98	.28	101.0
.58	2.32	.28	121.0
.63	2.5	.28	153.0
.92	3.0	.28	189.0
.84	2.4	.435	193.0
.82	3.11	.435	240.0
1.32	3.3	.435	280.0
1.41	1.38	.085	117.0
2.23	1.93	.085	133.0
2.23	2.03	.085	149.0
.86	1.72	.125	88.0
1.38	2.06	.125	133.0
1.96	2.15	.125	151.0
2.25	2.3	.125	181.0
.45	2.0	.28	109.0
.65	2.37	.28	137.0
.96	2.6	.28	161.0
1.25	3.1	.28	185.0
.75	2.55	.435	131.0
1.22	3.11	.435	181.0
1.23	3.1	.435	250.0

```

60 FORMAT(5X,19HSTANDARD DEVIATION=,F10.5)
   COV=(STD/CKAVG)*100.0
   PUNCH70,COV
70 FORMAT(5X,25HCOEFFICIENT OF VARIATION=,F10.5)
   DO80I=1,N
80 YN(I)=CKAVG*Z1(I)*Z2(I)*Z3(I)
   PUNCH90,(Y(I),YN(I),I=1,N)
90 FORMAT(2F15.5)
   S1=0.0
   S2=0.0
   DO100I=1,N
   S1=S1+Y(I)
   S2=S2+YN(I)
100 CONTINUE
   AN=N
   YM=S1/AN
   YNM=S2/AN
   SY=0.0
   SYN=0.0
   DO110I=1,N
   VY=ABS(Y(I)-YM)
   VYN=ABS(YN(I)-YNM)
   SY=SY+VY**2
   SYN=SYN+VYN**2
110 CONTINUE
   CAN=1.0-(SYN/SY)
   PUNCH10,CAN
   CAN1=SORTF(CAN)
   PUNCH120,CAN1
120 FORMAT(/,5X,34HMULTIPLE CORRELATION COEFFICIENT =,F15.5)
   STOP
   END

```

67

0.26	1.68	.125	36.0
1.17	1.98	.085	120.0

-----ALL THE SIXTY SEVEN DATA CARDS HERE AS PLACED IN
PROGRAMME NO. 1 -----

0.96	2.1	.125	42.0
1.11	2.33	.125	55.0

C	C	ME	THESIS	ISHWAR	CHANDRA.	CHEMICAL	UOR
		.00047		.00058		.00058	.00072
		.00071		.00057		.00061	.00067
		.00073		.00131		.00104	.00116
		.00057		.00123		.00093	.00103
		.00080		.00067		.00053	.00050
		.00054		.00083		.00114	.00125
		.00103		.00107		.00096	.00076
		.00088		.00096		.00080	.00075
		.00168		.00092		.00110	.00103
		.00118		.00092		.00109	.00097
		.00109		.00093		.00105	.00098
		.00111		.00098		.00179	.00167
		.00101		.00088		.00073	.00050

.00151	.00105	.00081	.00147
.00121	.00089	.00151	.00182
.00126	.00145	.00138	.00113
.00233	.00149	.00120	

CKAVG= .00102
 STANDARD DEVIATION= .00036
 COEFFICIENT OF VARIATION= 35.31694

.26000	.56253
1.17000	2.04875
.88000	1.54043
.80000	1.13178
.61000	.87614
.66000	1.18383
.28000	.47076
.47000	.71462
.68000	.95261
.71000	.55402
.79000	.77348
1.19000	1.05110
.15000	.27025
.52000	.43284
.54000	.59049
.24000	.23772
.28000	.35911
.32000	.49000
.16000	.30594
.22000	.45179
.27000	.50822
.64000	.78711
.84000	.75114
.72000	.58822
.39000	.38728
.57000	.57312
.88000	.94123
1.00000	1.34123
.35000	.40833
.58000	.60126
.63000	.80263
.92000	1.25580
.84000	.51082
.82000	.91016
1.32000	1.23145
1.41000	1.39286
2.23000	1.93876
2.23000	2.48928
.86000	.80643
1.38000	1.45201
1.96000	1.83515
2.25000	2.47909
.45000	.43823
.65000	.68008
.96000	.88724
1.25000	1.30473
.75000	.42792
1.22000	.74452
1.23000	1.24369
.52000	.60090
.65000	.91106

.38000	1.19347
.48000	.32378
.50000	.48639
.57000	.72005
1.85000	1.28957
2.33000	1.97342
2.33000	2.66722
1.20000	.81235
1.98000	1.11933
1.70000	1.37660
1.00000	.70477
1.80000	1.33411
2.08000	1.88412
.90000	.39401
.96000	.65947
1.11000	.94646
.09373	

0 MULTIPLE CORRELATION COEFFICIENT =
 STOP END AT S. 0120 + 01 L. 2

.30616